Werner Reichardt

Zentrum für Integrative Neurowissenschaften

Systemische Neurophsyiologie

Pavlovian eye blink conditioning (EBC) and learning-related activity in primary sensory neocortex

Inaugural-Dissertation
zur Erlangung des Doktorgrades
der Medizin

der Medizinischen Fakultät
der Eberhard Karls Universität
zu Tübingen

vorgelegt von

Zhang, Yuechen

2024

Dekan: Professor Dr. B. Pichler

1. Berichterstatter: Professor Dr. C. Schwarz
2. Berichterstatter: Professor Dr. B. Antkowiak

Tag der Disputation: 22.10.2024

Contents

0 Abbreviations

CR	conditioned response
CS	conditioned stimulus
CSD	current source density
DEBC	delay eye blink conditioning
DZ	dysgranular zone
EBC	eye blink conditioning
ISI	interstimulus interval
ITI	intertrial interval
LFP	local field potential
mPFC	medial prefrontal cortex
PBS	phosphate-buffered saline
POm	posterior nucleus
PSTH	peristimulus time histogram
S1	primary somatosensory cortex
TEBC	trace eye blink conditioning
TG	trigeminal ganglion
TN	trigeminal nuclei
UR	unconditioned response
US	unconditioned stimulus
VPM	ventroposterior medial nucleus

1 Introduction

1.1 Associative learning

During associative learning, an organism learns about the relationship of one stimulus to another stimulus or to the organism's behavior. Associative learning includes two types of learning progress named 'classical' and 'operant conditioning'.

In operant conditioning, the possibility of one behavior is increased by reinforcements and decreased by punishments contingent (in time and space) with the behavior.

Classical conditioning, also known as Pavlovian conditioning, generates the association of a neutral conditioned stimulus (CS) and a contingent behaviorally relevant unconditioned stimulus (US). US is defined as a stimulus that reflexively leads to an unconditioned response (UR), whereas a CS would not normally cause such a response. After repeated CS-US pairings, during which the US is regularly presented in a certain temporal relationship to the CS, the animal learns to predict the relationship between events and the CS can then elicit a conditioned response (CR), which resembles the UR. In the original experiment conducted by Pavlov (Fig. 1), the CS was the ringing of a bell, and the US was food, which reflectively triggered the dog's salivation (UR, Fig. 1A). After repeated pairing of CS and US (Fig. 1B), the dog acquired the association between the sound and the food, as indicated by the fact that it began to salivate in response to the sound alone (CR, Fig. 1C) (Pavlov 2010).

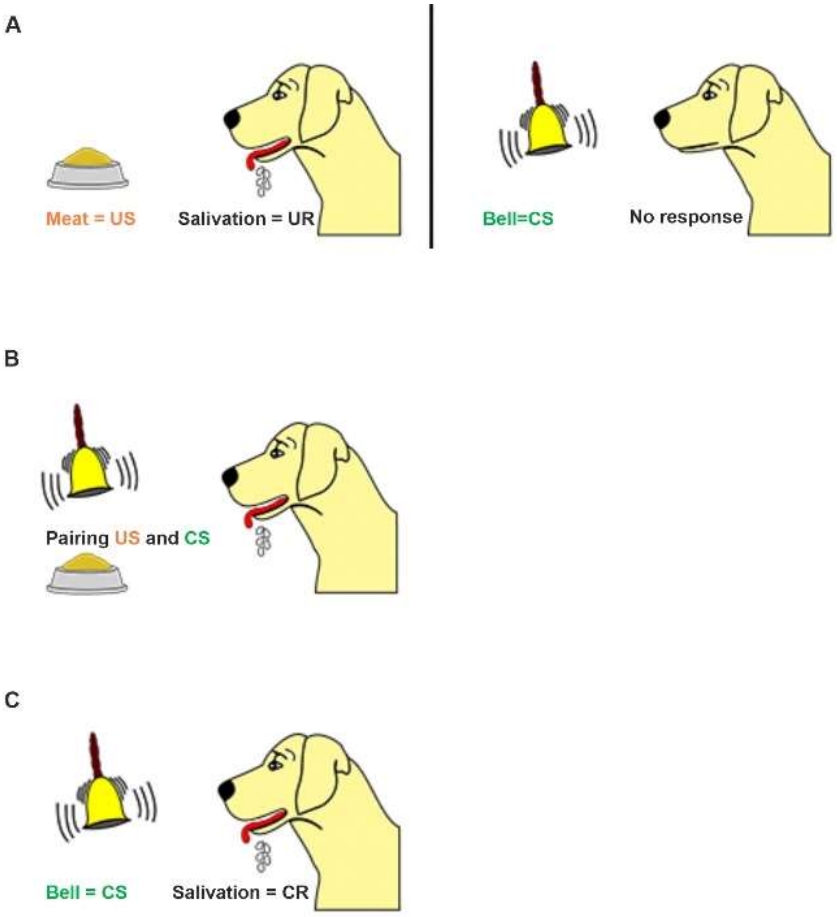

Figure 1. The original experiment of Pavlovian conditioning. **A** Before training, the dog salivated in response to food (US) and showed no response to the ringing of the bell (CS). **B** During training, CS and US are paired in the way that the bell sound was presented shortly after food representation. **C** After successful training, the dog acquired the association between CS and US (and UR) and started to generate a CR, i.e. it salivated after presenting the bell sound (CS) alone.

There are two common forms of classical conditioning, the 'delay' and the 'trace conditioning'. In the delay paradigm, the US is presented shortly after the onset of CS, overlaps and co-terminates with the CS. The trace conditioning paradigm was also first introduced by Pavlov, in which the presentation of CS and US is temporally separated by a stimulus-free interval, such that a 'memory trace', hence the name, is required to associate the two stimuli.

1.2 Eye blink Conditioning

Eyeblink conditioning (EBC) is a widely used model to study the neural principles of classical conditioning and has already revealed plenty of underlying neural mechanisms (Thompson et al. 1997).

In the eyeblink conditioning paradigm, the unconditioned stimulus (US) typically is either a corneal air puff or electric shock near the eye, triggering a protective reflex, an eye closure as an unconditioned response (UR). The conditioned stimulus (CS) is a stimulus of any sensory quality, typically auditory, visual, or somatosensory. Among those modalities, whisker deflection in rodents was established as a proper somatosensory CS in previous work, showing an advantage in examining the neural circuitry due to the characteristic 1-to-1 organization of individual whisker to columnar cortical structures, termed ‘barrel cortex’ (Woolsey and Van der Loos 1970; Galvez et al. 2006; Feldmeyer et al. 2013), which will be explained later.

After repeated pairing of CS and US, the reflex conditioning is acquired when the organism closes the eye after CS onset, but before US onset. The conditioned response (CR), an eyeblink upon presentation of the CS, was shown to be somewhat different from the unconditioned response (UR), as well as from spontaneous eyeblinks, in its kinematic properties, such as latency, velocity, and duration, and its neural basis (Ivkovich, Lockard, and Thompson 1993; Gruart, Blazquez, and Delgado-Garcia 1995; Gruart et al. 2000; Schade Powers, Coburn-Litvak, and Evinger 2010).

There exist delay eyeblink conditioning (DEBC) and trace eyeblink conditioning (TEBC) paradigms corresponding to the mentioned two forms of classical conditioning. In DEBC the US typically begins 200ms to 500ms after the onset of the CS and terminates together with the CS. In TEBC the stimulus-free interval typically ranges from 250ms to 1000ms between the end of CS and the onset of US (Fig. 2A). TEBC usually takes longer to acquire, and the involved learning and memory systems, and brain structures differ from those engaged in DEBC (Ivkovich, Paczkowski, and Stanton 2000; Beylin et al. 2001).

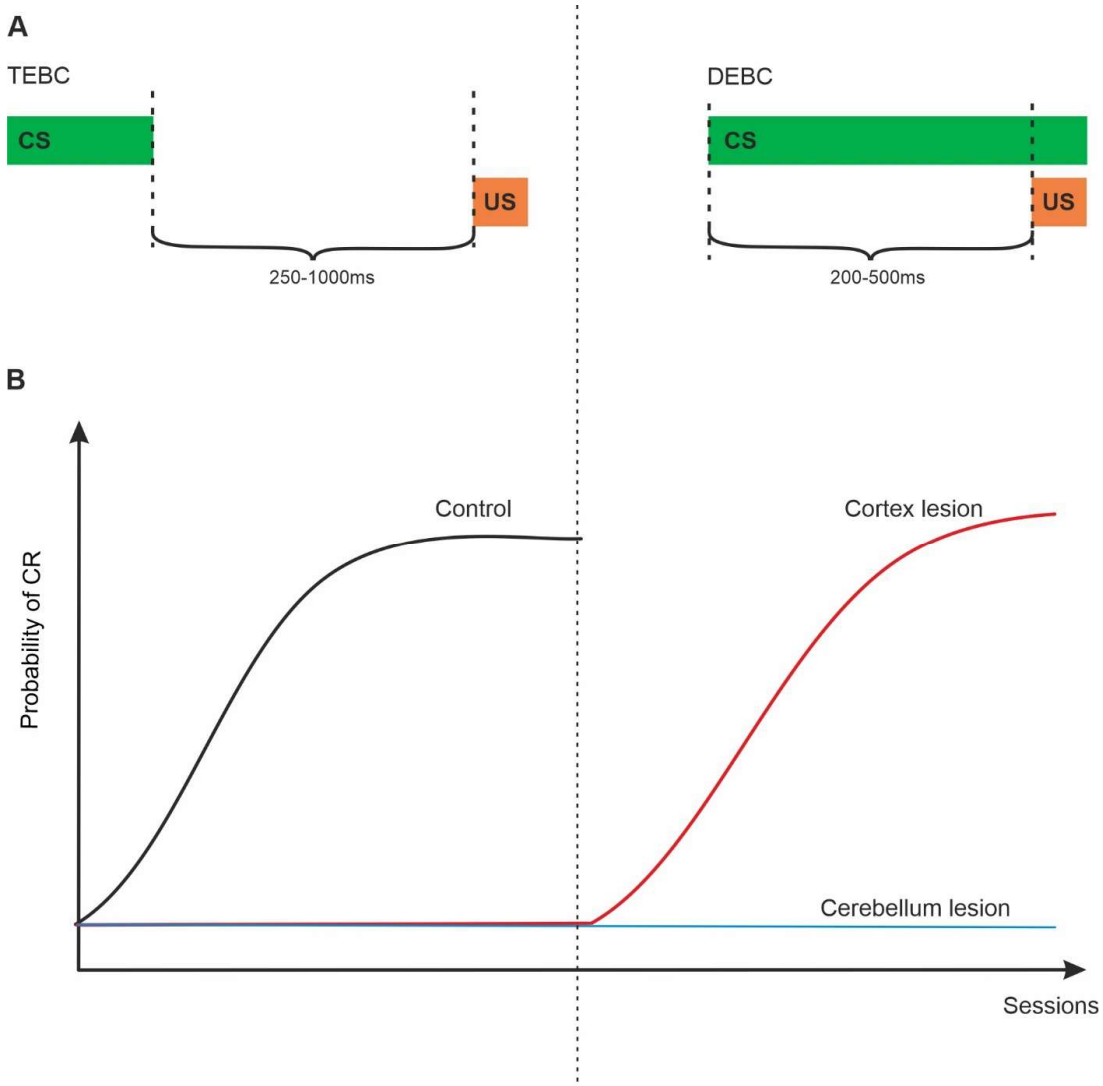

Figure 2. A Temporal relationship of CS and US in DEBC and TEBC. **Left:** In TEBC, the presentation of CS and US is temporally separated with a stimulus-free interval, which is usually around 250-1000ms. **Right:** In DEBC, the US is presented shortly after the onset of CS and the most commonly used time difference is around 200-500ms. The US overlaps and co-terminates with the CS. **B** Different brain structure involvements in DEBC and TEBC. The graphic illustrates the relationship of CR-probability with the number of training sessions. The control group (black curve) without any lesion of brain structures shows increasing CR-probability after training. Individuals with cortex lesions (red curve) are able to acquire DEBC (on the right side of the dotted line) but not TEBC (on the left side of the dotted line). Individuals with cerebellum lesions are able to acquire neither DEBC nor TEBC (Takehara-Nishiuchi 2018).

1.3 Implicit and explicit learning

Different learning and memory systems can be involved in the associative learning process. The implicit learning, also termed as procedural or nondeclarative learning, is generally regarded as unconscious and difficult to be described in words by humans. Comparatively, the explicit learning, also called declarative learning, requires consciousness in humans, and can be described in words. It is generally accepted that implicit learning depends on subcortical structures and does not necessarily require cortical involvement, while cortical structures are required for explicit learning (Fig. 2B). Implicit and explicit learning systems are also assumed to exist in rodents. Although their state of consciousness is undefined and cannot be examined through lingual expressions, they possess all the relevant brain structures that are believed to underly implicit and explicit memory in humans such as the neocortex, basal ganglia, cerebellum, and show similarities in the involvements of those structures in the implicit and explicit learning tasks.

An interesting question is whether the two learning and memory systems could work together in some circumstances.

The reflex conditioning, a relatively simple model of associative learning, is commonly regarded as an implicit learning process that is unconscious, automatic, and thus, the learned response assumes somewhat the quality of a reflex itself. Taking one of the best-studied reflex conditioning paradigms, the EBC, as an example, it has been proposed that DEBC do not require contingency awareness (Perruchet 1985; Manns, Clark, and Squire 2001; Clark, Manns, and Squire 2001), and acquisition of DEBC only depends on a brainstem-cerebellar circuit based on studies with decerebrated, decorticated rabbits or rabbits with lesions of certain cerebral structures (Oakley and Russell 1977; Mauk and Thompson 1987; Kronforst-Collins and Disterhoft 1998; Powell and Churchwell 2002). However, awareness influences the acquisition of TEBC (Clark and Squire 1998; Manns, Clark, and Squire 2000b, 2000a; Clark, Manns, and Squire 2001) and cerebral structures such as thalamus, hippocampus and medial prefrontal cortex are essential for TEBC learning to bridge the stimulus

free interval (Solomon et al. 1986; Moyer, Deyo, and Disterhoft 1990; Kronforst-Collins and Disterhoft 1998; Weible, McEchron, and Disterhoft 2000; Powell and Churchwell 2002; McLaughlin et al. 2002; Takehara, Kawahara, and Kirino 2003; Tseng et al. 2004; Oswald et al. 2006). The primary somatosensory cortex (S1) could also be required for both acquisition and retention of TEBC and might be a site for long-term-storage of associations (Galvez et al. 2006; Galvez, Weible, and Disterhoft 2007a; Joachimsthaler et al. 2015). Therefore, TEBC is now commonly regarded as a model for explicit learning, while DEBC is commonly assumed to be a model for implicit learning. The different characteristics of DEBC and TEBC acquisition raise the possibility that implicit and explicit learning are not necessarily engaged in isolation or as an alternative, but that they could simultaneously be involved in reflex conditioning even under conditions of DEBC, which classically has been considered as engaging only implicit/procedural learning (Thompson et al. 1997).

Several insights have suggested such an interaction. Interestingly, lesions of the hippocampus (a cerebral cortical structure) impair learning in DEBC, if the interstimulus interval (ISI) between the onset of CS and US is longer than 1s (Beylin et al. 2001). Manipulating awareness about the relationship between stimuli, using a paradigm called differential delay eyeblink conditioning, has been shown to affect the subjects' performance in the delay paradigm. Differential delay eyeblink conditioning presents an additional CS (CS-) that is not paired with the US, as well as the standard conditioned stimulus (CS+), paired with the US, requiring the subject to focus its attention to differentiate CS- from the CS+ (Weidemann, Satkunarajah, and Lovibond 2016). Another study suggested that the cerebellum could be sufficient to support the slow acquisition of TEBC with a relatively short trace interval and the cerebral structures could modulate and facilitate the learning process and are essential for TEBC with a longer trace interval (Li et al. 2019).

Taking all together, both learning processes could take part in either delay or trace conditioning, depending on the complexity of task demands or temporal relationships of the stimuli. Therefore, the present project tested whether

cerebral cortical structures show plasticity phenomena already under relatively simple DEBC conditions.

1.4 Whisker-related tactile system in rodents

Whiskers, mobile sensory hairs on either side of the snout, act as tactile sensors enabling the rodents to explore the environment, detect and locate objects, discriminate texture and shapes, navigate, and find food. As mentioned above, the well-studied rodent whisker-related tactile system with a highly resolved, 'barrel-like' cortical organization representing predominantly a single whisker offers an ideal model to study the possible involvement of the primary somatosensory cortex in the context of reflex conditioning. For TEBC, the involvement of barrel cortex plasticity in the learning process has already been shown (Joachimsthaler et al. 2015).

In short, the rodent whisker system is organized as follows: The mechanical vibration of the whisker is transduced into neuronal signals by end-organs of primary afferents in touch with the hair's shaft and papilla inside the specialized whisker follicle. Primary afferents are characterized by axonal structures that conduct action potentials toward their somata in the trigeminal ganglion (TG), a structure close to, but still outside the brain. From there, the neural signals are carried further via a second (efferent) axon to the trigeminal nuclei in the brainstem. Primary afferents contact only one whisker. Thus, they show strict mono-whisker responses. This is different in the trigeminal nuclei, in which cells exist that already integrate signals across whiskers but with longer latencies as compared to those responsive to only a single whisker (Veinante and Deschenes 1999; Minnery, Bruno, and Simons 2003). Still, the trigeminal nuclei contain histological zones, the barrelettes, each representing predominantly one whisker (Woolsey and Van der Loos 1970; Ma and Woolsey 1984). The next station is the thalamus, especially the ventroposterior medial nucleus (VPM), again with histological zones predominantly related to one whisker, called barreloids. The posterior nucleus (POm), however, while receiving inputs from the trigeminal nuclei, does not show such zones (Veinante and Deschenes 1999; Minnery, Bruno, and Simons 2003). VPM barreloids are subdivided into

head, core, and tail – each defining a separate ascending tactile pathway, called lemniscal and extra-lemniscal – with the core receiving input from single-whisker cells in the brainstem, while the head and tail respond to more than one whisker (Brecht and Sakmann 2002b; Furuta, Kaneko, and Deschenes 2009). VPM core replays the tactile signals to the barrels, again histologically visible structures, responding primarily to one principal whisker, limited to layer 4 of the primary somatosensory cortex (S1). Each barrel is associated with the barrel columns spanning the entire depth of the cortex, from superficial layer 1 to deep layer 6 (the limits of the barrel column are not visible in histology). The head and tail of thalamic barreloids, as well as POm, relay the tactile signals also to cortical areas outside the barrel columns within S1 (Fig. 3, 4), as well as to wide-spread targets in the parietal cortex, and even motor cortex (Feldmeyer et al. 2013).

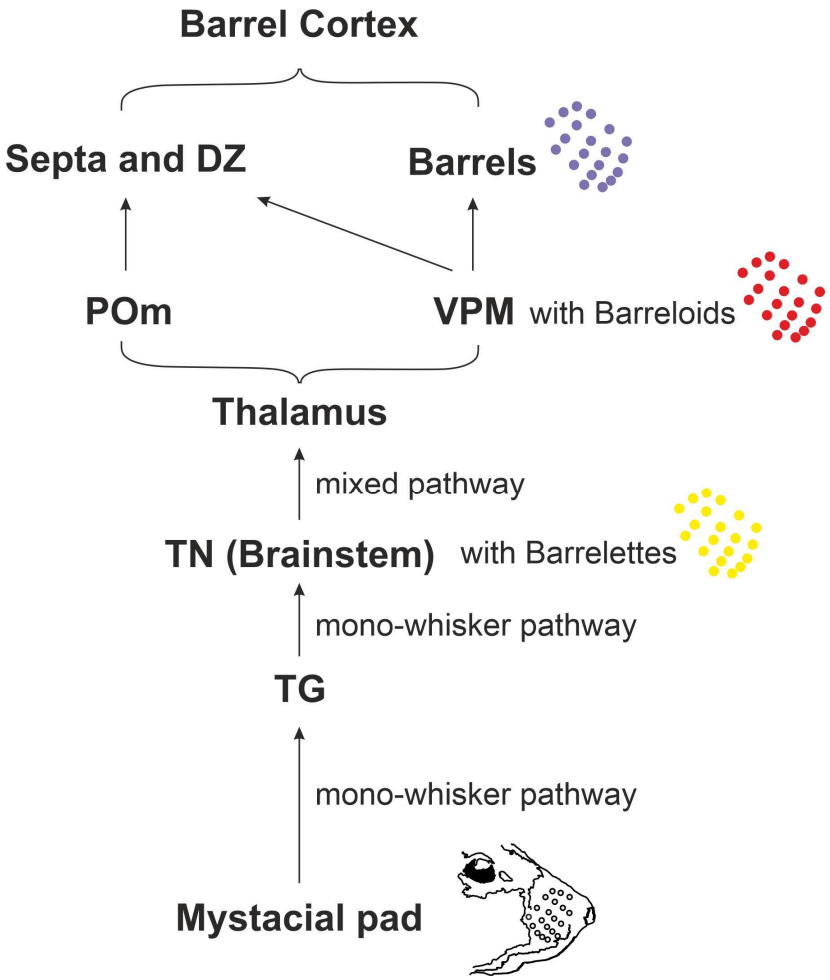

Figure 3. An outline of the neural ascending pathways in rodent whisker-related tactile system. The neural signals evoked by deflection of mystacial whiskers are projected to the somata of the primary afferents (tactile receptor cells) in the trigeminal ganglion (TG). From TG the neural signals are then projected to the trigeminal nuclei (TN) in the brainstem. In primary afferents the neural signals are carried in mono-whisker fashion (i.e. one primary afferent responds exclusively to one whisker). However, neurons in TN barrelettes (schematic as yellow dots) represent already more than one whisker, with one whisker having the strongest response (principal whisker). In ventroposterior medial nucleus (VPM) the histological zones called barreloids (schematic as red dots) also respond predominantly to one whisker. Another thalamic nucleus, the posterior-medial nucleus (POm), however, does not show such zones. From the thalamus nuclei the signals are sent to cortical areas in the primary somatosensory cortex (S1). Barrels (histological structures in layer 4 of S1, schematic as purple dots) receive signals of predominantly one whisker from corresponding barreloids in VPM. Multi-whisker signals are conducted from VPM and POm to regions located in between the barrels and associated barrel columns, the so called septa and dysgranular zones (DZ) (Feldmeyer et al. 2013).

The so-called ‘barrel field’ in S1 represents the array of contralateral whiskers in the array of barrel columns separated by cortical areas called septa columns (‘septa’) and dysgranular zones (DZ) (Fig. 4A). The inputs of a barrel column from the different thalamic nuclei are complex (Woolsey and Van der Loos 1970; Crockett et al. 1995; Veinante and Deschenes 1999; Veinante, Lavallee, and Deschenes 2000; Furuta, Kaneko, and Deschenes 2009; Wimmer et al. 2010; Wright and Fox 2010; Ohno et al. 2012). Nevertheless, the overall arrangement is that a barrel column receives the most precise inputs, mainly from one principal whisker via the respective barreloid (Woolsey and Van der Loos 1970; Welker 1976; Land and Simons 1985), while septa and DZ receive more diffuse multi-whisker signals from different origins including VPM, POm, and other cortical areas. In this way, the topographical order of the whiskers on the snout is principally kept on the ascending pathways in form of the principal whiskers of brainstem barrelettes, thalamic barreloids and cortical barrel columns. It is also noticeable that longer whiskers have larger corresponding barrels and barrel columns (Welker 1976). Thus, stimulation of the so-called E1 vibrissae, a large whisker, whose barrel column in S1 is conveniently located on the dorsal surface of mouse neocortex, was chosen to be located using intrinsic imaging (see Material and Methods) and utilized for recording neuronal signals during learning in the present experiments (blue in Fig. 4B).

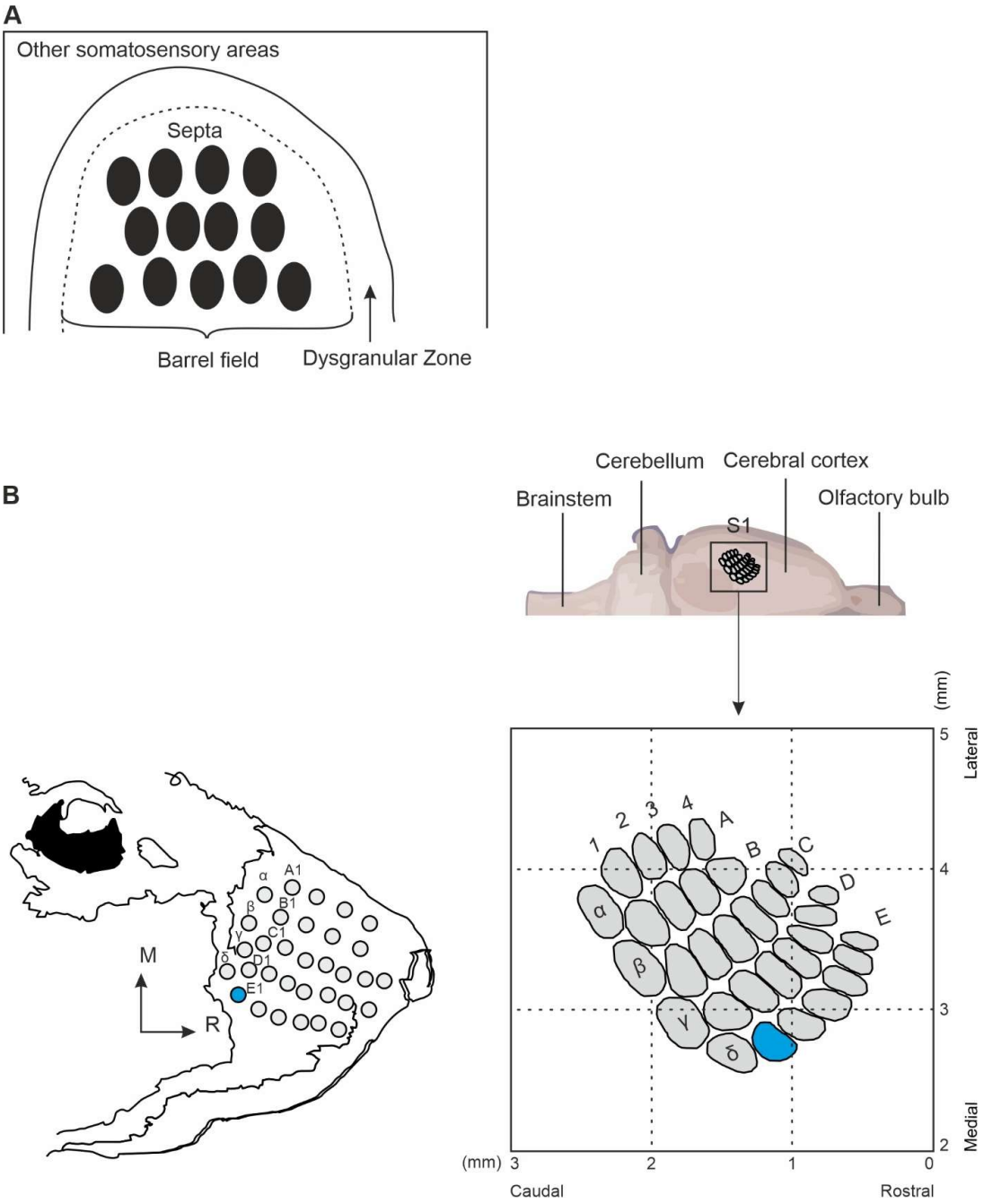

Figure 4. A schema of barrel field structure consisting of barrel column, septal column and dysgranular zone. Black dots illustrate schematically the barrel columns. The dotted curve marks the border of barrel field and the white area below the dotted curve illustrates septa that separate the barrels from each other. The white area between black and dotted curves illustrates the dysgranular zone that separates the barrel field from other somatosensory areas. **B Left,** schema of mouse whisker pad on the right side of face. **Right,** a schema of the left hemisphere of mouse brain from the top with marked rough position of S1 barrels corresponding to the whiskers on the right face. The graphic shows the topography of the barrels. The scale in millimeter marks the relative position of the barrels from bregma, the intersection of the sagittal and coronal sutures, on the scull.

1.5 Aim of the study

The explicit and implicit learning mechanisms may coexist in a learning process, with the latter one resulting in motor actions, such as lid movements in eye blink conditioning, while the former one is involved in the formation of knowledge about the contingency. As already mentioned, several cerebral structures are required for TEBC. A detailed study of the involvement of these cerebral structures in DEBC could be a starting point for revealing the link between implicit and explicit learning.

This study focused on the primary somatosensory cortex (S1) and aimed at finding out whether there are any learning-related plasticity changes during the DEBC learning process. A corneal air puff was used as unconditioned stimulus (US) and a single whisker deflection as conditioned stimulus (CS). Stimulation of the E1 whisker was performed while recording in the E1 barrel column. As it is well-established that DEBC is independent of cortical function (Fig. 2), the finding of learning-related neuronal activity would be the first evidence that explicit learning may play a role in parallel to implicit learning to the DEBC learning process.

Eyelid responses across trials were registered to obtain learning scores reflecting learning progress. To demonstrate plasticity, extracellular multi-unit spike recording was performed via a chronically implanted microelectrode array in the barrel column of head-fixed awake-behaving mice. This way the highest experimental control throughout training and data collection was ensured (Schwarz et al. 2010). Instead of comparing a group of conditioning learning and a control group of pseudo-conditioning as often has been used in previous studies, this study attempted to find the dynamic, trial-resolved, within-individuum relationship between the learning curve and neurometric data, taking into consideration that learning curves can differ substantially from one individuum to the next. This dynamic relationship is defined as ‘learning-related activity’.

2 Material und Methods

2.1 Animals

All experimental and surgical procedures were performed in accordance with guidelines of animal use of the Society for Neuroscience and German Law (approved by the Regierungspräsidium Tübingen). Adult male wildtype C57BL/6 mice were housed individually with food and water ad libitum under an inverted 12h light/dark cycle. Training sessions were conducted during the daytime (i.e. within the active period of the nocturnal mice).

2.2 Surgery

Animals received oral antibiotics (Baytril®, Bayer Vital GmbH, Germany) for 3 days before the surgery. The implantations were conducted under general anesthesia (fentanyl 0.05 mg/kg, midazolam 5.00 mg/kg, medetomidin 0.50 mg/kg, i.p.). To protect the eyes from drying out during the surgery, moisturizing ointment was applied (Bepanthen®, Bayer Vital GmbH, Germany). A homeothermic pad was utilized to maintain the body temperature at 37°C. Local analgesic (Xylocaine®) was applied on the shaved and disinfected skin. A skin incision was performed, and the connective tissue and bone were also locally anesthetized. The skin was carefully deflected, the connective tissue scraped off, and the scull cleaned with 3% hydrogen peroxide solution. Then the scull was coated with a light curing bond (Optibond® FL, Kerr GmbH, Germany) and a thin layer of dental cement (Tetric® Evoflow, Ivoclar Vivadent AG, Liechtenstein). Two silver balls were placed onto the surface of the cerebellum and prefrontal cortex through two small trepanations. They served as ground and recording references.

To locate the barrel column corresponding to the E1 whisker, intrinsic optical imaging was utilized (Masino et al. 1993; Joachimsthaler et al. 2015). Principally, light is shown on the surface of the cortex, and its reflection is captured by a CCD camera. An active cortical area obtains more flow of oxygenated blood and causes ion and water movements, neurotransmitter release, and expansion and contraction of extracellular spaces, which in sum result in different light reflection properties compared to inactive areas. This was detected by the CCD

camera and visualized as two-dimensional images by software. A 2×2mm area of the scull over the barrel cortex (0mm-2mm caudal to bregma, 2mm-4mm lateral to bregma), was thinned for the intrinsic optical imaging. With the CCD camera, the pattern of the surface blood vessels was captured under green light (570 nm) as a reference. The intrinsic optical signal was captured under monochromatic red light (630nm) with the camera focusing on a cortical depth of 200 –250µm. At the same time, a whisker was inserted into a piezo element tube and deflected at a 5mm distance from the face (60 Hz sine wave, 0.7mm rostrocaudal amplitude). The captured images were processed with the software HelioScan (Langer et al. 2013). The area activated by the whisker stimulation was automatically detected by the boxcar filter with a kernel of 10×10 pixels. The range of the captured gray values was then normalized to [0, 255] and a threshold was adjusted for the activation area with an approximate diameter of a barrel (300µm) (Fig. 5A). The same procedure was repeated several times for E1 and its adjacent whiskers to ensure the reliability of the results. At the end, the imaging results were merged into one picture showing the relative location of each whisker in reference to the surrounding blood vessels (Fig. 5B).

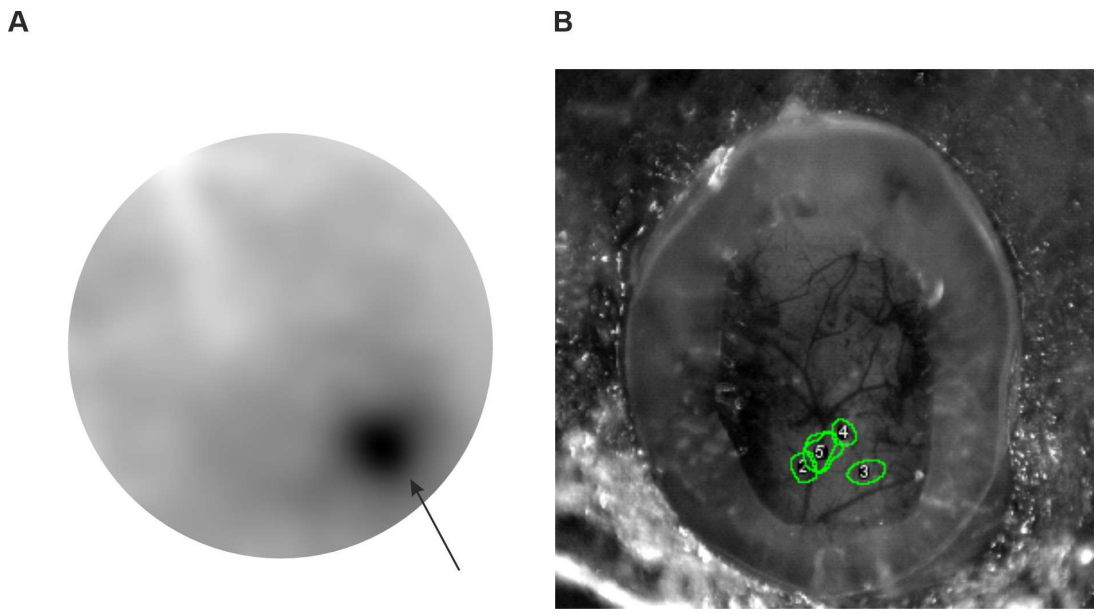

Figure 5. Intrinsic optical imaging. **A.** Raw data of intrinsic imaging (an example which does not correspond to the merged image in B). The black spot marked by the arrow shows the area stimulated by whisker vibration. **B.** Merged picture after software analysis showing the blood vessels (black lines) and the spots (green circles) each representing one whisker (the overlapping numbers 1 and 5 both represent E1, and number 2-4 represent adjacent whiskers). The green circles correspond to neighboring barrel columns and have a diameter of about 300 µm.

After identifying the location of the E1 barrel column, the thinned scull was removed, without damaging the dura mater, for the implantation of a microelectrode array. The electrodes were implanted perpendicular to the surface of the cortex and were lowered to a depth of around 350µm. To protect the electrodes from being blocked by the dental cement, which is applied to fix the array on the head-cap, silicone sealant (Kwik-Seal ®, World Precision Instruments, USA) was used to fill the space between the electrodes. A metal cylinder was placed covering the array for protection and was also fixed onto the head-cap with dental cement. A 10mm M3 screw was cemented head-down onto the head-cap for the head fixation. Silver paint electric shielding was applied in the way that the cylinder contacts the ground pins on the plug of the implanted silver balls but not the pins of the electrodes.

After suturing the skin, anesthesia was terminated by an antidote (naloxone 1.20 mg/kg, flumazenil 0.50 mg/kg, atipamezol 2.50 mg/kg, s.c.). Analgesia was assured by injecting carprofen (0.05 mg/kg/d, s.c.) before antagonizing the anesthesia and continued throughout 3 postoperative days. Animals received oral antibiotics (Baytril®, Bayer Vital GmbH, Germany) for two weeks postoperative and were allowed to recover from surgery for minimally one week before the experiment was started.

2.3 Behavioral Training

Head-fixed awake-behaving mice (Fig. 6) were used as subjects of the study based on the following reasons: Firstly, the head-fixed animal offers a highly precise experimental control over sensory inputs and motor outputs. In the EBC paradigm, the US (air puff on the eye) and CS (whisker stimulation) can be precisely controlled both temporally and spatially, and the motor output, the eye closure, can be precisely registered by an optic sensor. Secondly, the electrophysiological signals are less affected by the artifacts caused by the movement of the animals compared with freely moving preparations. And in comparison with anesthesia preparations, the possible anesthesia effects on cerebral function can be avoided (Schwarz et al 2010).

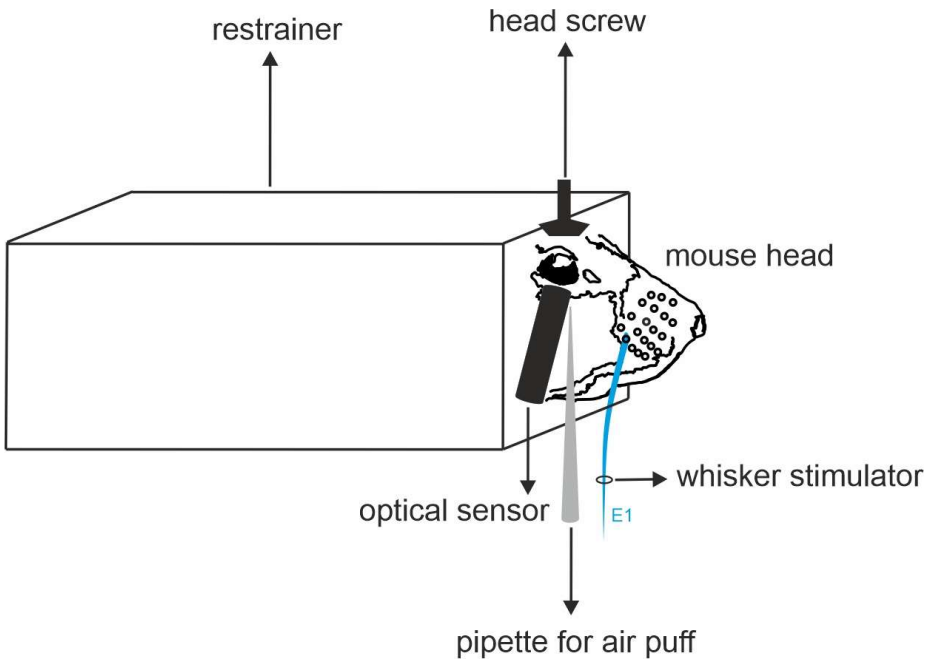

Figure 6. Schematic of a head fixation setup (demonstrated objects are not to scale). The mice are restrained by a screw implanted on the head cap that can be fixed onto the restrainer. The E1 whisker (blue) was inserted into a whisker stimulator (black circle). An air-puff pipette (grey cone) was placed at about 3mm, and an infrared optic sensor (black cylinder) at about 2mm from the eye.

Before training, the mice (n=7) were habituated to the head fixation and the experimental setup for 2 weeks on average, guided by the behavior and stress level of each individuum (Schwarz et al. 2010). At the end of habituation, the mice were comfortable to be get used to head-fixation in a restrainer box and staying in a dark environment with white noise for about 30min with whisker insertion into a galvo-motor, optic sensor, and air puff pipette positioned close to the eye. The mice were trained 1 session per day, lasting for about 30 minutes, and in total for at least 5 subsequent days always at the same time of the day until the acquisition of DEBC. By always providing a similar context (same time, same experimenter, identical lab environment), the influence of the animals' varying states (wakefulness, concentration, satiation, etc.) on behavioral learning and data collection was intended to be minimized.

A daily session consisted of 60 paired CS-US trials, separated by a randomly varied intertrial interval (ITI) of 20-40s (mean interval of 30s). The CS was a 250-ms-long single sinusoidal deflection of whisker E1 (60 Hz sine wave, 5° position amplitude, 1870°/s velocity amplitude) delivered by a galvo-motor (6210H Galvanometer Scanner & analog servo driver 677XX; Cambridge Technology), followed by the US that began 200ms after CS-onset, lasted for 50ms and terminated together with CS. The US was a corneal air puff ipsilateral to the deflected whisker around 2mm distant from the eye with a thin 200µl pipette at 40psi. Eyeblinks were monitored by an infrared light source and sensor (OPR5005, Optek, TT Electronics, England) that translates the eyelid movements into a voltage signal (Weiss and Disterhoft 2008; Joachimsthaler et al. 2015) (Fig. 7).

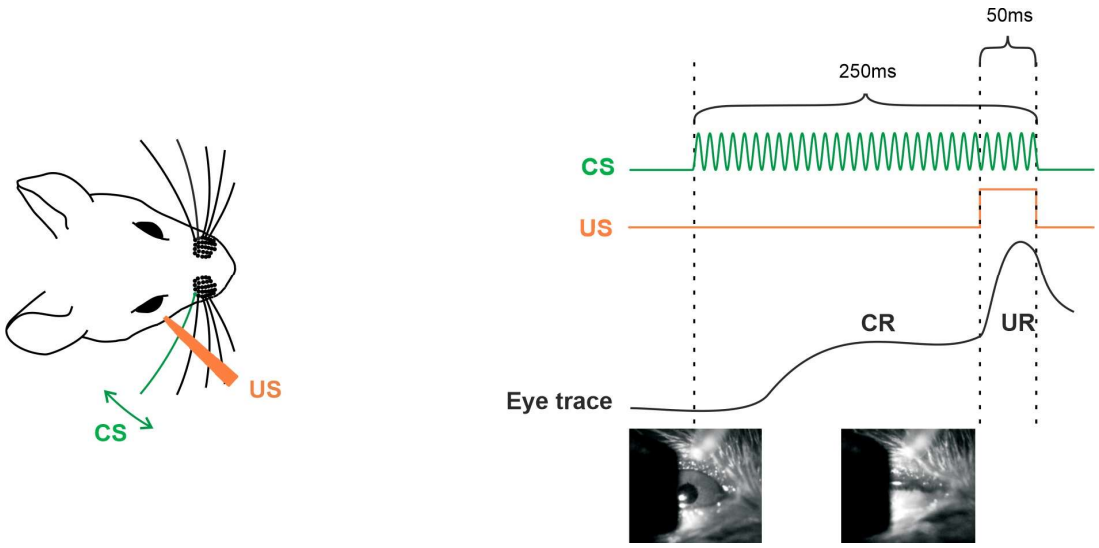

Figure 7. An outline of DEBC behavioral training. **Left,** sinusoidal movement of a single whisker (60 Hz, amplitude 5°) was applied to head-fixed mice as CS, while an air puff against ipsilateral cornea was applied as US (40psi). **Right,** the duration of CS (green line) was 250ms followed by an overlapping 50-ms US (orange line) that co-terminated with CS. After successful acquisition of the contingency, the mice generated eyelid movements in response to whisker stimulation (CR) captured by optic sensor as eyelid trace (black line, schematic) with lower amplitude compared to the coming UR after US-onset.

Throughout the habituation and training session, white noise sound (60 dB) was presented to mask potential acoustic emissions of the whisker stimulator.

After each habituation and training session, the mice were rewarded with food.

2.4 Construction of individual trial-resolved learning curves

The eyelid traces of each trial were analyzed and classified into three categories: CRs, non-CRs, and invalid eyelid movements (closed eyes). If the voltage shortly before CS onset was similar with the voltage of a UR, the eyelid trace was classified as closed eyes and invalid. CRs were defined as eyelid traces with significant voltage increases (at least 20% of the UR voltage) during the CS presentation which should last for the rest time of the trial until the US presentation. A valid eyelid trace which did not fulfill the criteria of a CR was then classified as non-CR. After manual validation of the eyelid trace dataset with a custom-made MATLAB software, further classification of CRs and non-CRs was conducted by a one-dimensional convolutional neural network (CNN, TensorFlow version 2.0, Python software). The CNN was comprised of three convolutional layers and three neural layers with dropout regularization to prevent overfitting and used 2109 manually labeled eyelid traces of previous behavioral experiments for training. 15% (n=316) out of the 2109 eyelid traces were manually classified as invalid and excluded from the dataset for training. The estimated accuracy of the neural network after training was 94.2%. The classification with CNN was manually double-checked with a semiautomatic MATLAB software. CNN and manual monitoring software were written and provided by May Li Silva Prieto, another doctoral student in the lab (Silva-Prieto, Hofmann, and Schwarz 2023).

The raw data of the learning process was presented by a binary vector (non-CR=0, CR=1) with bins corresponding to the trials. To smooth out short-term fluctuations and highlight long-term trends, moving averages of the binary data were generated with a kernel width of 9 trials (Fig. 9, grey lines). Assuming that disturbing factors such as forgetting or distractions of the animals are negligible, the learning progress is supposed to be described by a monotonically increasing function. The monotonic curve was approximated by accepting increasing learning scores but ignoring falling scores. In the latter case, the curve would keep the value of the last score. The upper-bound, monotonic learning curves created this way are shown as black lines in figure 9. It is assumed that the trial-resolved learning of a single individual does not follow the

classical S-shaped learning curve, which rather is thought to be an artifact of group averaging (Gallistel, Fairhurst, and Balsam 2004). Instead, the cited study has shown that individual learning curves are characterized by an abrupt rise from the untrained level to the learned level within only a few trials. The Weibull function is commonly used to fit psychometric data sets that are monotonic and reflects the mentioned characteristics much better than the commonly used logistic curves. The advantage of the Weibull fit is that the shape of the resulting learning curve can assume highly variable shapes, depending on the value of parameters selected for the function, so that the various shapes of individual monotonically increasing learning curves can be properly fitted (Gallistel, Fairhurst, and Balsam 2004). Therefore, the upper bound curves mentioned before (Fig. 9, black lines) were fitted by the Weibull function resulting in a smooth description of learning (Fig. 9, curves in colors), as needed for the analysis in figure 11.

A learning score was defined by the number of CRs out of nine subsequent valid trials. It ranged between 0 (0 out of 9) and 1 (9 out of 9). The Weibull fit spans the same range of learning scores.

2.5 Electrophysiology

Seven adult male wildtype C57BL/6 mice were implanted with a chronic wire electrode array (lab produced; 4-shank, spatial arrangement of a 2×2 matrix, fiber diameter approximately 80µm, distance between electrodes approximately 250µm; made of quartz glass fiber with a metal core purchased from Thomas RECORDING GmbH, Article No. An000125, Germany) for the recording of extracellular neuronal activities during the acquisition of DEBC (Haiss, Butovas, and Schwarz 2010).

The electrodes were implanted in the E1 barrel column at a depth of around 350µm on the day of surgery and were later advanced to a depth of around 850µm, corresponding to layers 4 or 5, where spikes could be observed during whisker stimulations. The advancement was performed one day before the start of training so that the tissue was stabilized at the time of recording.

Two separate head-stage amplifiers were used for spike and local field potential (LFP) signals. In each mouse recorded in this study, there could be found one electrode that did not show high amplitude spike waveforms (i.e. 50μV and higher). This electrode was used as a reference for the recording, as it would very reliably remove movement artifacts from the recordings (movement artifacts would appear in identical form in all electrodes, and therefore were calculated out when referencing the spike-containing recordings to the recording of the spike free recording).

2.6 Spike Analysis

The raw data of electrophysiology recordings were band-pass filtered (Butterworth filter, edge frequencies 500 and 3000Hz; filter passband ripple amplitudes < 0.5dB, stop-band attenuation > 30dB). With a MABLAB software (lab written), the threshold for extraction of multi-unit spikes across sessions was semi-automatically adjusted for each individual and each electrode, yielding a firing rate of 30Hz from pre-stimulus spontaneous activities. All spike rates used in the results referred to the difference between the evoked spike rates during the trial and the pre-stimulus spontaneous firing level.

2.7 Statistics and Quantification

2.7.1 Weibull function

The Weibull function was utilized to fit the smooth learning curve. The following cumulative distribution function was selected for the purpose:

$$F(x;k,b) = 1 - e^{-(x/\lambda)^k}$$

In the function, k is the shape parameter and λ is the scale parameter of the distribution, which were adjusted to generate a function that best fit the learning curve of each subject.

2.7.2 Regression analysis

Regression analysis was used for estimating the relationship between neuronal activity changes and learning progression. A linear function was chosen for the analysis:

$$Y = \beta_1 X + \beta_0$$

Y was the dependent variable (spike rates), X was the independent variable (learning score), and β1 referred to the slope.

Simulink/Matlab (MathWorks R2014b for behavioral training and R2020a for data analysis) was utilized to conduct experimental control and analysis. HelioScan was utilized to conduct Intrinsic optical imaging (Langer et al. 2013).

2.8 Histology

To examine the exact location of implanted electrodes, the animal was perfused with fixative, to produce histological slices.

Before perfusion, the position was marked by electrochemical lesioning using 10μA current passing through the electrode (duration of 10s, repeated for 2-3 times) in deep anesthesia.

The perfusion was conducted according to lab protocol. In brief, the mice were euthanized with Pentobarbital (100ml/kg). To perform brain-targeted perfusion, the major blood vessels (thoracic aorta and vena cava inferior) to the lower body were occluded with curved hemostats. A perfusion needle was inserted into the left ventricle and the right atrium was clipped. The animals were then perfused continuously at a slow rate with 4% paraformaldehyde (about 3-5cc) until the blood was replaced with clear perfusate. After perfusion, the brain was removed carefully from the scull and stored in 20% sucrose solution for 24h at 4 °C. After 24h the brain was washed with phosphate-buffered saline (PBS) and then stored in 0.1M PBS at 4 °C.

After sectioning (60μm) on a cryostat, and subsequent CO staining (Chakrabarti and Schwarz 2018) the histological slices were studied under the microscope, and the location of the implanted electrodes was identified (Fig. 8).

Figure 8. An example of a brain slice showing the location of implanted electrode in S1. Area between two dotted lines illustrates barrel cortex with barrel columns. The arrow shows the electrode implantation pathway with a lesion spot showing the location of the electrode. This brain slice shows that the electrode located roughly at a depth between L4 and L5.

3 Results

Seven mice m1-m9 (m6 and m7 were eliminated from the dataset because of postoperatively broken electrodes) were trained on the DEBC paradigm for at least 5 sessions (60 trials per session) on subsequent days. Specifically, a 250ms deflection of E1 whisker (CS, 60 Hz sine wave, 5° position amplitude, 1870°/s velocity amplitude) was paired with a corneal air puff ipsilateral to the deflected whisker (US, about 2mm distant from the eye, 40psi). The acquired response to CS (CR) was defined as significant eyelid movements to the extent of at least 20% of the UR and lasting until US-onset. The eyelid movements were detected by an infrared light source and sensor.

The mice [m1, m2, m3, m4, m5, m8, m9] were labeled by consistent colors [red, orange, sky blue, blue, magenta, green, yellow] in figures 9 to 11.

3.1 Behavioral learning

For each mouse [m1, m2, m3, m4, m5, m8, m9], there were [263, 363, 282, 276, 497, 251, and 231] valid eyelid traces/trials throughout the entire training. The number of (CR, non-CR) were [(239,24), (261, 102), (146, 136), (110, 166), (87, 410), (176, 75), (152, 79)]. Defining a learning score from 0 (no learning) to 1 (complete learning; see Materials and Methods), the maximum learning score for each mouse throughout the total training sessions was [1, 1, 0.98, 0.87, 0.74, 0.99, 1].

The individual behavioral learning progress is shown in figure 9 by trial-resolved learning curves. All learning curves tended to rise abruptly as expected from previous findings (Gallistel, Fairhurst, and Balsam 2004). But at the same time, the curves also show that learning rates differ strongly among subjects. Mouse m1 and m2 were fast learners while m5 was relatively slow in picking up. The onset latency of CRs, however, was not strictly related to the asymptotic level of the learning score. For example, m3 and m9, which started to generate CRs relatively late, readily reached learning scores similar to the ‘fast learners’ m1 and m2. The trial at which the Weibull fit reached its steepest slope coincided well with that of either the raw learning curve or the extracted monotonic one

(gray and black lines in Fig. 9) so that the nature and timing of abrupt onset of learning is captured well by the Weibull fit.

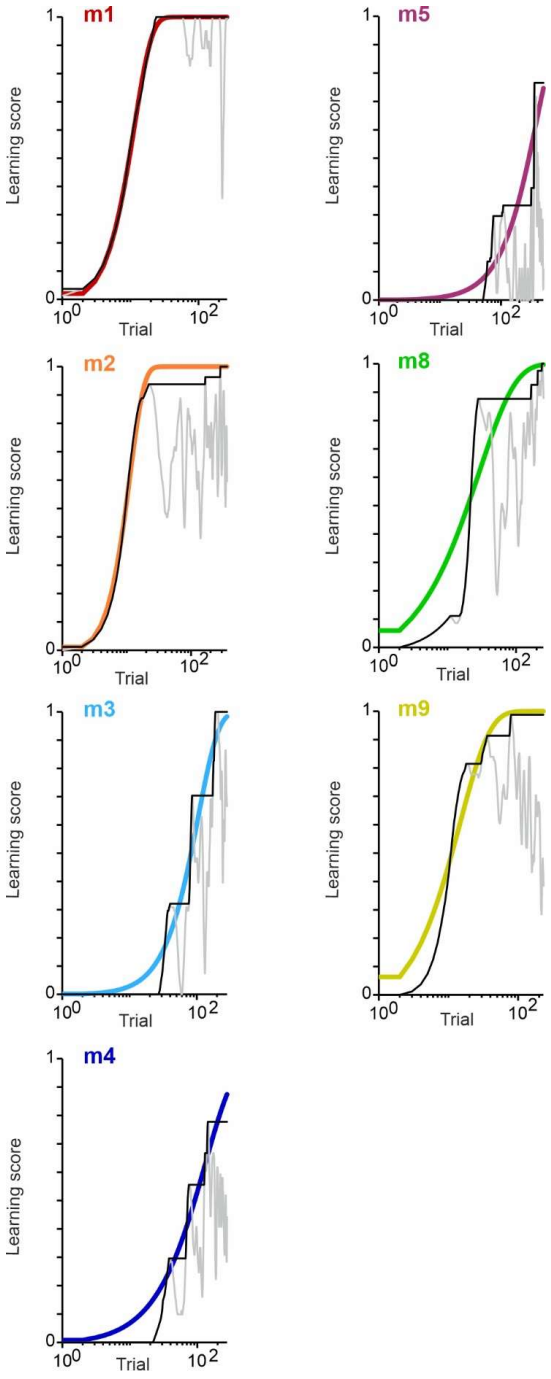

Figure 9. Learning curves of seven trained mice (coded with different colors). X-axis is trial number and y-axis is learning score. The gray line is a moving average (kernel width 9 trials) of the binary raw data (CR=1; non-CR=0). The black line is a monotonic upper bound, generated by tracking the increment of the moving average, but keeping the value constant if the moving average decreases. The curves in different colors illustrate Weibull fits to the upper bound learning curve (black curves). The colors are consistent in figures 9-11.

3.2 Averaged neuronal firing pattern across trial time

For the registration of extracellular neuronal activities during DEBC learning, the mice were implanted with a 4-shank (2×2) chronic wire electrode array. The arrays were implanted in a way that they were centered on the E1 barrel column as visualized by intrinsic imaging. All electrodes were thus within or in the immediate vicinity of barrel column E1 (Joachimsthaler et al. 2015).

The spike rates were computed as the difference between firing rates during the trial and during the pre-stimulus period and were averaged across shanks, excluding the reference shank. The average spike rates across the entire trial time of each animal are presented as peristimulus time histogram (PSTH) (Fig.

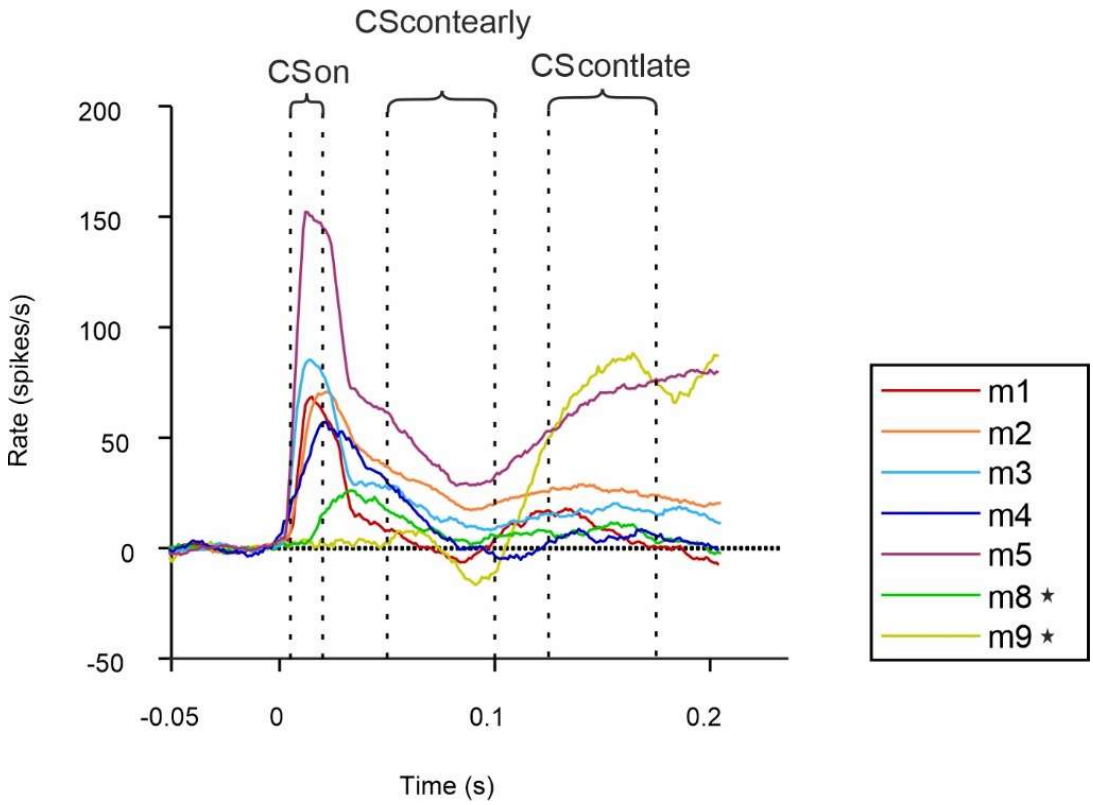

Figure 10. Peristimulus time histogram (PSTH) about spike rate changes related to trial time. 0s on the x-axis is the timing when CS began and 0.2s is when the US began. The spike rate referred to the difference in firing rate during the trial and during the pre-stimulus period and was averaged across shanks and across all trials. Note the short-latency excitatory response directly after the CS-onset and the following firing suppression during the CS presentation. The spike rates in three epochs CSon (5-20ms), CScontearly (50-100ms), and CScontlate (125-175ms) will be further studied with regression analysis below. The asterisk marks the outliers showing different firing patterns and different activity changes across learning (presented below in Fig. 11). The colors are consistent in figures 9-11.

10).

Shortly after the onset of whisker stimulation (CS), a short-latency onset response of around 7ms was observed in 5 out of 7 mice, consistent with previous results (Chung, Li, and Nelson 2002). The amplitude of the onset response varied among the subjects. The maximal response is shown by mouse m5 (purple curve, Fig. 10). The onset responses of mouse m8 and m9 were outliers within the data set, but also with respect to the literature (Stuttgen and Schwarz 2008). The response of m8 (green curve) showed a longer latency and in m9 (yellow curve) none of the electrodes captured a response. LFP data showed typical short-latency responses (around 5-7ms) as a negative deflection in all mice except for m9 (because of high variability across trials, the LFP data was not used for quantitative analysis and thus not presented here).

Adapted firing after the onset response reached a minimum at about 100ms after the CS onset. Again, mouse m5 showed the highest level but the ranking of the other subjects did not correspond to that of the onset response. During this period of suppressed firing rate, there was a concave trajectory visible with variation in all subjects, leading to an enhanced firing rate toward the onset of the US. Interestingly, mouse m9 (yellow curve), which did not show the onset response, showed the described late firing rate trajectory in a pronounced way.

In sum, the pattern of spiking was similar across mice, except for m8, which showed a delayed onset response in the spikes (not LFP), and m9, which entirely lacked an onset response. The lack of onset response in m9 is unclear, as later responses during the CS were similar to the results in other mice. As the implant, electrodes and recordings in mice m8 and m9 did not show an obvious technical failure, the data were marked as outlying but were kept within the data set (Fig. 10)

3.3 Learning-related changes of neuronal activity in S1

To further study learning-related neuronal activity changes, the spike rate was plotted in relation to the learning score (from 0 to 1) as taken from the y-axis of the learning curve (fitted Weibull function) in figure 9. Linear regression analysis

was utilized to estimate the relationship between the changes in neuronal activities and learning progress (Fig. 11A). The spike rate was again averaged across the electrodes of an array and the data were processed for each mouse individually.

The neuronal activity change was studied in three epochs: CSon (5-20ms), CScontearly (50-100ms), and CScontlate (125-175ms) (all intervals with respect to CS onset). In CSon and CScontearly intervals, the linear regression showed negative slopes in most subjects except for m8 (green line) and m9 (yellow line). In the CScontlate phase, the slope of m8 turned to be negative, while the slope of m9 remained positive. All other subjects showed negative slopes in CScontlate. The slopes for each individuum in the three epochs are shown in figure 11B. The grand averages of the slopes among all the subjects in each of the intervals, CSon, CScontearly, and CScontlate, were -68, -43, -31. The mean slopes (diamonds) in all the three epochs were negative, strongly indicating a suppression of firing rates in all phases of CS presentation during DEBC acquisition learning.

The distribution of slope values across animals is presented in figure 11C. Panels B and C together show that within the data set, there was a strong preponderance of firing rate suppression with learning score. The outlying mice m8 and m9 were the only ones that showed deviant responses. The correlation between firing rate and learning success is noteworthy and is the main result of this project – it is termed learning-related responses. It is a first-step evidence supporting the notion that S1 neuronal firing undergoes plastic changes during DEBC learning.

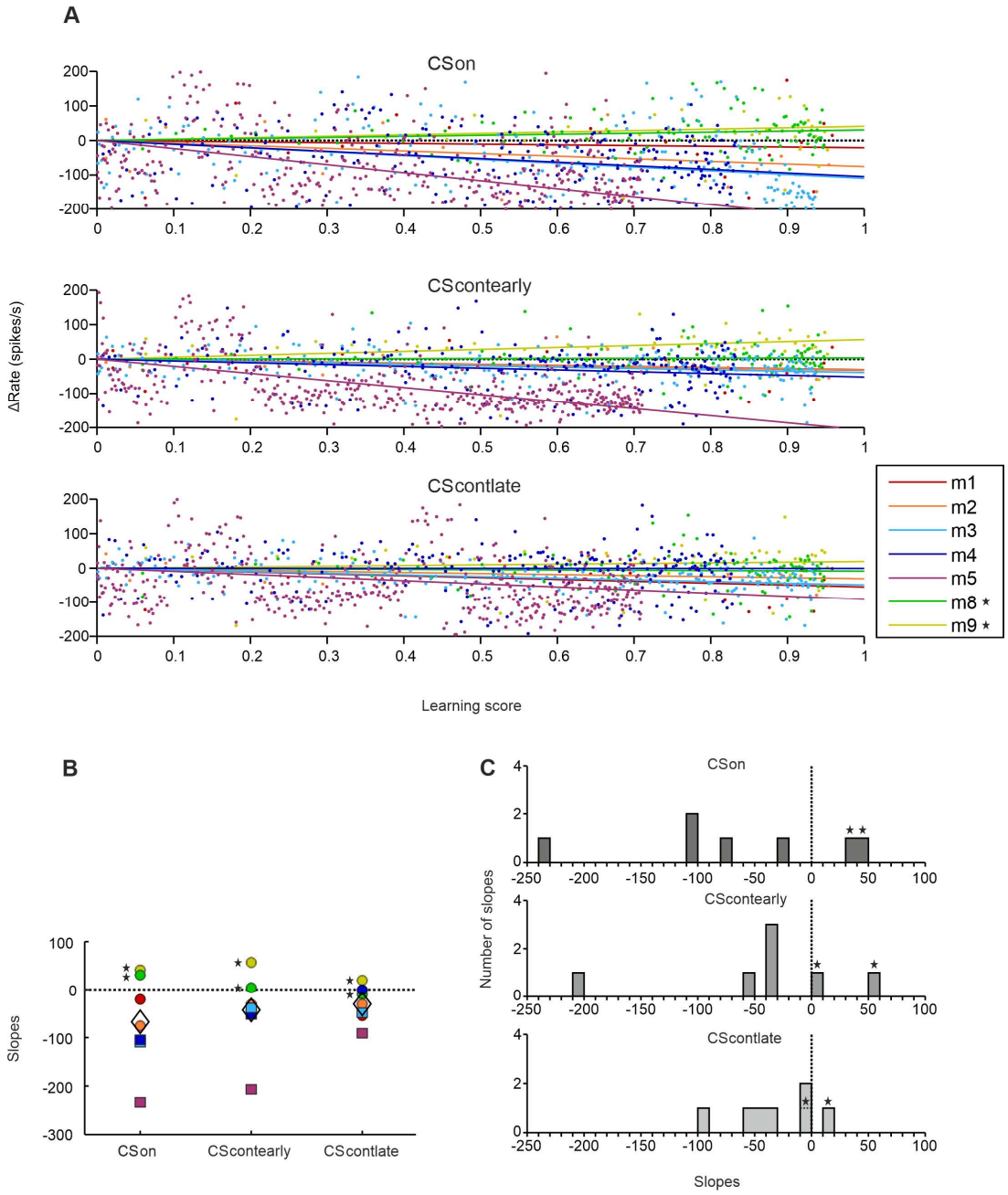

Figure 11. Changes in spike rate (Δ Rate) across learning progress. **A.** Spike rate averaged across shanks was plotted in relation to learning score of each individuum and for three epochs (CSon, CScontearly, CScontlate). Each dot represents spike rate in one certain trial and the x-coordinate of the dot is the learning score of this trial according to the smoothed learning curve. Linear regression was generated for each mouse. To ease comparability the y-axis intersection was slightly shifted and set to 0. **B.** Slopes of the regression line of each mouse (colored circles with $p>0.05$; colored squres with $p<0.05$) was shown, reflecting firing rate changes across the entire learning process (learning score from 0 to 1). The mean slope of all subjects was plotted as diamond. **C.** Distribution diagram of the slopes of all the animals in the three phases. Note that most slopes were distributed in the negative area. The colors are consistent in figures 9-11. The asterisk marks the outliers as mentioned above in Fig. 10.

4 Discussion

In this study, the neuronal activity change in the primary somatosensory cortex during DEBC acquisition learning was examined. Within a single individual, the learning curve was compared to the trial-resolved multiunit spike rates recorded in the barrel column that corresponded to the stimulated whisker. The results suggest that there is a learning-related firing suppression during the CS presentation and support the possibility that the primary somatosensory cortex might play a role in some aspects of Pavlovian eye blink conditioning. The fact that previous work has shown that learning of CRs is independent from cerebro-cortical function (Fig. 2), opens the possibility that the learning-related activity observed here is related to another learning system, perhaps the explicit learning of contingencies.

4.1 Methodological aspects

4.1.1 Intensity of CS and US stimuli

The training paradigm utilized single sinusoidal whisker deflection (60Hz, 5° position amplitude, 1870°/s velocity amplitude) as CS and corneal air puff (40psi) about 2mm distant from the eye as US. These stimuli intensities are identical to those utilized in the recent study of barrel cortex involvements in TEBC (Silva-Prieto, Hofmann, and Schwarz 2023).

As mentioned in the Results, some mice showed eye blink responses in early trials, and one of them (m1) showed an eye blink response even in the first trial. The sinusoidal whisker deflection used here (amplitude 5°, maximal velocity 1870°/s) is surely detectable. Previous data in rats (Stuttgen, Ruter, and Schwarz 2006), showed that in the regime of amplitudes larger than 3°, a single whisker deflection can already be detected at velocities as low as around 125°/s. The master's thesis of Lili Rötzer (2022) conducted in the lab (after the present data had been recorded) suggested that conditioned responses occur earlier and more frequently when using whisker stimulation of higher intensity. Moreover, she noted that higher deflection intensities can generate eyeblinks by itself, however with low probability. It can, therefore, not be excluded that in the

mice with very early responses the estimate of the learning curve was shifted somewhat to earlier trials. There is no good reason to assume that this potential bias would have led to an overestimation of the negative slopes of learning-related activity. On the contrary, it may have been the reason that in these mice (m1, and m2) the negative slope of learning-related activity was not captured as well as it could have been because the learning-related activity did occur later than indicated by the shifted learning curve. Matching this reasoning, the two mice in question (m1, m2; red and orange colors in Fig. 11B) did show moderate, but clearly negative slopes, i.e. they still captured the effect despite the possible shift in the learning curve. These considerations do not apply to the mice with a slower onset of CR generation.

The US used here (40psi air puffs) was clearly suprathreshold and generated robust URs. Rötzer's work (2022) also showed that the intensity of the air puff (US) can influence the learning speed. Utilizing the same DEBC paradigm as in this study (60Hz, 5° whisker deflection), a 10 or 20psi air puff led to acquisition after the first few trials, while the learning speed was much lower when using 5psi and 10psi air puff. In conclusion, the high intensity of CS and US used in this study further facilitated DEBC acquisition. The present result, as well as the ones reported by Rötzer, are in line with previous studies, which have suggested that emotional learning is a regular part of EBC (Taub and Mintz 2010), with the amygdala amplifying the sensory (CS) input to the cerebellum, such that the amygdala contributes to the first phase of learning with fast CRs, while cerebellum is contributing to the second phase of learning with more slow and deliberately timed CRs (Lee and Kim 2004; Boele, Koekkoek, and De Zeeuw 2010; Sakamoto and Endo 2010; Siegel et al. 2015).

An approach to reduce possible non-associative eye blinks occurring in response to the whisker stimulus in further studies, is to reduce the intensity of the whisker deflections (CS) and/or air puff (US). Pre-exposing the animals to the stimuli by performing a series of pseudo-conditioning trials before starting the conditioning training could be another way to reduce such responses (Manns, Clark, and Squire 2001). An advantage of this approach would be that

the electrophysiological data sets during pseudo-conditioning could be compared with data acquired during learning. A severe disadvantage of this procedure, however, might be that it has been reported to lead to latent inhibition, slowing or even preventing learning (Puga et al. 2007; Miller et al. 2022).

4.1.2 Location of recording

Histological confirmation of recording sites was hampered by the movement of the electrode through the tissue leading to clearly visible tracks but obscuring the histochemical lesions. In fact, in this study the recording site of only one mouse (m2) could be found (Fig. 8). Therefore, reliable reports of the depth of recordings in terms of cortical layers for the current data set could not be secured. This may be the reason for the outlier results obtained in mice m8 and m9. In terms of horizontal misplacement (along the surface plane of S1), intrinsic imaging is supposed to be a reliable method to guide electrode placement: always barrel columns E1, as well as several neighboring columns (E2, D1, and б) were imaged repeatedly (Fig. 5) to confirm the result and to exclude spurious signals. The patterns obtained by intrinsically imaging these barrel columns were consistent in all mice (across repetitions as well as in comparison of the known maps of the barrel field; cf. the map shown in Fig. 4B). Therefore, the error margin of the site of electrode implantations along the surface of the cortex can be safely assumed to be very small. Future approaches may benefit from using multi-electrode silicon-based arrays placing electrodes at regular locations throughout the depth of the cortex. This will allow the computation of a current source density (CSD) map, which contains very reliable signatures of the depth of recording (Nicholson and Freeman 1975; Mitzdorf 1985; Silva-Prieto, Hofmann, and Schwarz 2023).

For the two mice that did not show the classical ON response (m8 and m9), several possible scenarios can be discussed. Firstly, the array may have been placed such that only columns neighboring to the one connected to the principal whisker were stimulated. This possibility is unlikely because, as discussed, the horizontal placement guided by intrinsic imaging is safe. Even if, e.g. due to

cortical curvature, a slight misplacement occurred, the effect should have been minor as barrel columns in fact respond to many adjacent whiskers with minor delay differences (Chmielowska, Carvell, and Simons 1989; Ghazanfar and Nicolelis 1999; Harris, Petersen, and Diamond 1999; Manns, Sakmann, and Brecht 2004; Feldmeyer et al. 2013; Silva-Prieto, Hofmann, and Schwarz 2023). The overlap of broad receptive fields and the spread of signals to neighboring columns are supported not only by the integration of ascending multi-whisker projections but also by trans-columnar processing that plays a prominent role for barrel columns to receive multi-whisker signals (Armstrong-James and Callahan 1991; Armstrong-James, Callahan, and Friedman 1991; Goldreich, Kyriazi, and Simons 1999; Brecht and Sakmann 2002a; Fox et al. 2003; Wright and Fox 2010).

A second problem could have been that only inter-barrel columns were recorded. This possibility is negligible, as inter-barrel columns in mice are very narrow (tens of microns) (Feldmeyer et al. 2013) such that the placement of the 2x2 array (with electrode distance 250µm) exclusively into inter-barrel space is impossible.

A further possibility is a cortical microlesion in the surrounding area of the implanted electrodes. However, since the neuronal signal was intact and the response to later phases of the CS was present, the potential lesion should have selectively severed the inputs to the barrel column, a scenario that seems unlikely.

Finally, it is noteworthy that in addition to the aberrant or missing CSon responses, these mice (m8 and m9) also lacked learning-related activity (i.e. they showed positive slopes of learning-related activity or slopes very close to zero, cf. Fig. 11). This correlation gives cause to think that these mice are true outliers. Amongst the five other mice (m1, m2, m3, m4, m5) the results were clear-cut and unique: strong onset responses were paired with consistently negative slopes of learning-related activity. Future experiments also including pseudo-conditioning or extinction learning will help to clarify this issue.

4.2 Learning-related neuronal firing suppression in barrel cortex

In this study, similar neuronal firing patterns and changes could be observed in five out of the seven mice across learning. As mentioned before, two mice (m8 and m9) showing deviating CS-onset spike response (m8: longer latency; m9: no CSon response) did not show decaying firing rates along with the learning progress.

The PSTH showed that the neuronal firing rate of each animal decreased to a level close to the spontaneous firing rate during CS presentation after a short-latency excitatory response. This decrease represents most likely cortical adaptation, a phenomenon that has been reported in many previous studies (Maravall et al. 2007; Stuttgen and Schwarz 2010; Wang, Webber, and Stanley 2010; Yang and O'Connor 2014; Waiblinger, Brugger, and Schwarz 2015; Gerdjikov, Bergner, and Schwarz 2018). The time course (a sharp decline within about 15ms after the beginning of the sensory response, reaching a low firing level within 100ms) and the extent of decrease (more than 80% in most of the subjects) observed in this study were approximately consistent with those reported before (Simons 1985; Chung, Li, and Nelson 2002; Webber and Stanley 2006; Maravall et al. 2007). Interestingly, the general firing pattern in later phases of the CS, as observed in this study, was highly consistent with previous studies including the slight elevation after firing depression (Ahissar, Sosnik, and Haidarliu 2000; Ahissar et al. 2001). However, it is worth noting that those studies were performed under urethane anesthesia, and the latency differences of CS onset responses shown in this previous work have never been able to be reproduced in awake mice (Stuttgen and Schwarz 2008; Silva-Prieto, Hofmann, and Schwarz 2023).

To further reveal the effect of learning on neuronal activity changes, the relationship between trial-resolved spike rates and learning score was examined with linear regression analysis, showing negative slopes in the five animals that displayed similar averaged firing patterns in the PSTH. Although not each individual regression function yielded a significant p-value, the overall

consistency of this finding indicated a general tendency of spike rate suppression during CS presentation across learning.

These findings are comparable with a recent study about learning-related neuronal activity changes during TEBC acquisition, in which a similar experimental design was utilized (Silva-Prieto, Hofmann, and Schwarz 2023). With respect to behavioral training, head-fixated mice, the same stimuli with the same intensity, and the length of CS-presentation (250ms) were used in identical ways. TEBC presented a 250-ms stimulus-free trace interval. Further, with respect to the method used to study neuronal plasticity changes, also multi-unit spike and LFP between L4 and L5/6 were registered and were studied trial-resolved and within-individuum. The study showed a similar firing rate suppression across learning with TEBC as shown here with DEBC. The result was less obvious in CSon (5-20ms), but comparable to the later intervals CScont (125-175ms) and Trace (375-475ms). Generally, therefore, the present results obtained here with DEBC are comparable to the ones obtained with TEBC. The correspondence is most obvious if one ignores the outlying results on CS response and learning-related decrease in later responses in mice m8 and m9. A difference in detail is that the previous study on TEBC reported the decline in firing rates predominantly in the later phases of the CS (and the trace period), while the present results suggest that learning-related changes occur throughout the CS presentation including CSon. This difference cannot be easily explained based on the present data. It needs to be consolidated and studied more in detail in the future.

4.3 Reconsidering the role of the cerebral cortex in reflex conditioning

It is generally assumed that reflex conditioning is an implicit learning process that does not necessarily require consciousness and cortical involvement. Nevertheless, the two typical forms of reflex conditioning, delay and trace conditioning, show different characteristics. Other than the delay paradigm that is considered to depend exclusively on subcortical structures, the cerebral cortex has been proposed to be essential for trace conditioning learning (Solomon et al. 1986; Moyer, Deyo, and Disterhoft 1990; Kronforst-Collins and

Disterhoft 1998; Weible, McEchron, and Disterhoft 2000; Powell and Churchwell 2002; McLaughlin et al. 2002; Takehara, Kawahara, and Kirino 2003; Tseng et al. 2004; Oswald et al. 2006). Although decortication or decerebration has been suggested not to impair delay conditioning learning in terms of acquisition rate (Oakley and Russell 1977; Mauk and Thompson 1987; Kronforst-Collins and Disterhoft 1998; Powell and Churchwell 2002), it was reported that decortication affects CR properties (onset latency and amplitude) acquired in delay paradigm (Oakley and Russell 1972, 1975). Therefore, already in classical work, a certain role of the cerebral cortex could not be finally excluded.

The above-mentioned effects of the amygdala, a neuronal structure in the cerebrum, -mediating emotional components, is a point in case, for which a facilitating effect on EBC learning has been shown (Lee and Kim 2004; Blankenship et al. 2005; Taub and Mintz 2010). As discussed, this effect could well explain the rapid acquisition observed in the present study using strong aversive stimuli and is consistent with previous observations of our lab (Rötzer 2022).

Other forebrain structures are likely involved as well in the modulation of delay conditioning learning. It was reported that medial septum lesions retarded DEBC (Berry and Thompson 1979; Allen, Padilla, and Gluck 2002). Moreover, lesions or inactivation of the medial prefrontal cortex (mPFC) decelerated the acquisition of delay conditioning if a soft tone was used as CS. Such inhibition was not observed during training with a loud tone as CS (Wu et al. 2012).

Similar phenomena were observed in the hippocampus: its lesion/inactivation inhibited DEBC acquisition when a soft tone was utilized, but not when a loud tone was used (Wu et al. 2013). Although hippocampus lesion or dysfunction was reported to neither impair nor facilitate delay acquisition (Weiskrantz and Warrington 1979; Lee and Kim 2004), it still has been reported to have effects on CR expression, such as onset latency and peak amplitude (Port, Mikhail, and Patterson 1985; Christiansen and Schmajuk 1992; Lee and Kim 2004). Moreover, neuronal activity changes in the hippocampus have been reported during delay conditioning training, and the patterns were reported to differ from

those observed in the trace paradigm (Green and Arenos 2007). On a side note, the hippocampus has been reported to affect DEBC learning, if the CS duration is increased above ~1s, in ways that are similar to those observed with TEBC using the same ISI (Beylin et al. 2001). This phenomenon, however, may find a possible explanation with the fact that a long CS duration effectively acts as a shorter CS followed by trace, due to strong cortical stimulus adaptation occurring along long intervals bringing the firing rate basically back to pre-stimulus levels.

Further findings suggested that the motor cortex affects delay conditioning learning in its acquisition and expression and disinhibits the primary somatosensory cortex by an intracortical circuit (Ammann et al. 2016; Umeda, Isa, and Nishimura 2019).

Concerning the somatosensory cortex (S1), the targeted cortical area in this study, most previous research focused on the TEBC paradigm. It has been suggested that S1 is essential for TEBC acquisition in that TEBC learning is impaired after barrel lesion (Galvez, Weible, and Disterhoft 2007b) and optogenetic blockade of the barrel cortex during the CS presentation (Silva-Prieto, Hofmann, and Schwarz 2023). Furthermore, plasticity changes in S1 have been reported during TEBC learning. Spine loss of layer 5 pyramidal neurons in the barrel cortex was observed (Joachimsthaler et al. 2015). In addition, an expansion of corresponding barrel columns several days after TEBC acquisition has been reported (Galvez et al. 2006), suggesting that S1 might be a site for storage of part of the memory trace of TEBC. It has been observed that post-acquisitional barrel lesions reduce the expression of already learned CR (decreased percentage of CRs; increased percentage of responses with smaller amplitude, earlier peak, and shorter duration terminating before US-onset) (Galvez, Weible, and Disterhoft 2007a). However, impairment of TEBC retention has not been confirmed by a recent study using optogenetic blockade (Silva-Prieto, Hofmann, and Schwarz 2023). Therefore, further studies are required to study the exact function of S1 during TEBC learning. In summary, the barrel cortex has been proven to be a critical structure for TEBC acquisition, while less information was obtained for the DEBC paradigm. In the

present study, the multi-unit spike recording showed a learning-related firing suppression which is comparable with what has been observed in the previous study of the TEBC paradigm (Silva-Prieto, Hofmann, and Schwarz 2023). The reduction of neuronal activity during TEBC is paralleled by spine loss of layer 5 neurons (Joachimsthaler et al. 2015). Whether this is true for the DEBC as well, remains to be examined in the future. There is one piece of evidence that the barrel cortex undergoes structural plastic changes during delay Pavlovian conditioning paradigm using tail shock as the US, showing that after a 3-day delay conditioning learning, the inhibitory synapses in L4 of the barrel cortex increase (Jasinska et al. 2010).

At present, it remains an open question, whether the plasticity of synapses is a cellular correlate of the firing suppression, and what functional role this plasticity change plays in the signal processing of sensory information. Interestingly, according to a previous study (Silva-Prieto, Hofmann, and Schwarz 2023), specific blockade exclusively during the trace period of TEBC, which in the same study has been suggested to contain a more significant firing suppression effect than during CS presentation, does not impair TEBC acquisition learning. This finding suggests that the observed learning-related spike suppression in the infragranular layer, however, rather represents other aspects of learning and is probably not essential for the acquisition of association in TEBC. In view of the similarity of firing rate suppression, the same can be hypothesized to be the case also for the here reported firing rate suppression during DEBC. It is noteworthy, that the S1 recordings in mice m8 and m9 lack a standard CSon response, and concomitantly do not show the firing rate suppression. This supports the notion that repeated stimulation by itself does not generate the firing rate suppression. In the future, this needs to be further tested using a group of mice trained on a pseudo-conditioning paradigm (Joachimsthaler et al., 2015), i.e. applying the same set of CS and US stimuli, but in non-contingent ways preventing the association.

Another supporting evidence for decaying firing rates during association learning comes from work focusing on a concept called ‘sparse coding’, which results in a decrement of network activity during association learning but not

during mere stimulus repetitions (Willmore, Mazer, and Gallant 2011; Gdalyahu et al. 2012).

4.4 Outlook

As discussed above, the cerebral cortex may take part in the learning process of EBC. For TEBC, the possibility that the memory trace is stored in S1 was rendered unlikely by the ineffectiveness of optogenetic blockade during the trace period (Silva-Prieto et al., 2023). Another argument that the memory trace that is stored in S1 is that learning-related results in DEBC, found here, parallel the ones reported earlier for TEBC, although during DEBC a memory trace connecting the stimuli is not needed. Alternatively, the S1 function during EBC may be to tune CR properties. This possibility needs to be further examined by studying the correlation of S1 plasticity changes (structural and electrophysiological) with latencies and movement parameters. Finally, S1 plasticity may as well be the expression of learning the task contingencies. Against this notion speak the previous findings that awareness of the stimuli contingency has significant effects on CR elicitation only in TEBC, but not DEBC (Papka, Ivry, and Woodruff-Pak 1997; Manns, Clark, and Squire 2000b, 2000a; Clark, Manns, and Squire 2001; Manns, Clark, and Squire 2001). These results have been obtained with human participants, where the awareness level could be tested and intervened e.g. by words or questionnaires. In the animal model, it cannot be tested in the same way. However, the fact that during explicit learning the probability of certain behavior positively correlates with higher predictions or expectations, while during implicit learning the probability of the behavior only reflects the strength of the stimuli association (Clark, Manns, and Squire 2001) may be used for an experimental design in mice as subjects so that the explicit component can be indirectly read out. More generally, to understand the role of S1 plasticity better, studies of plasticity not only across acquisition but also throughout memory consolidation and during extinction, will be helpful. In summary, the similarity of firing suppression observed during DEBC (this study), and during TEBC (previous study) lends support to the notion that they relate to the learning of the task contingency

forming explicit memory. However, more work as outlined in this paragraph will be needed to finally make this point.

5 Summary

Eye blink conditioning (EBC) is a widely used model to study the neural circuitry of classical conditioning and is commonly regarded as an unconscious, implicit learning process that exclusively depends on subcortical structures. However, humans can also describe task contingencies of reflex conditioning in words, a kind of explicit, declarative memory, provoking the consideration that even the simplest variant of reflex conditioning might involve the cerebral cortex, although many previous studies have shown that the procedural part of learning (i.e. the acquisition of CRs) is not impaired by decortication in delay conditioning, perhaps the simplest form of classical conditioning (see below) (Oakley and Russell 1977; Mauk and Thompson 1987; Kronforst-Collins and Disterhoft 1998; Powell and Churchwell 2002).

There are two forms of EBC, delay (DEBC) and trace (TEBC) eye blink conditioning. In DEBC the unconditioned stimulus (US) begins at a delay after the onset of the conditioned stimulus (CS) and co-terminates with it. In contrast, in TEBC there is a stimulus-free interval between the end of CS and the onset of US, which requires the formation of a memory 'trace' to associate the two stimuli. Several previous studies found that there are plasticity changes in the whisker representation of rodent primary somatosensory cortex (S1, barrel cortex) during TEBC learning (Galvez et al. 2006; Galvez, Weible, and Disterhoft 2007a; Joachimsthaler et al. 2015), while little was known about its involvement in DEBC. Therefore, this study aimed to identify spike rate plasticity in S1 as well during DEBC. If plasticity were to be found in S1 during DEBC in a similar fashion as known from TEBC, the finding would support the notion that it is the expression of explicit learning.

To this end, head-fixed awake-behaving mice were used to ensure the highest experimental control throughout training and data collection. A corneal air puff was utilized as the unconditioned stimulus (US) and E1 whisker deflection as the conditioned stimulus (CS). During the entire learning process, eyelid responses in each trial were identified and registered to obtain learning scores across trials reflecting the learning progress. To demonstrate the plasticity

changes, extracellular multi-unit spike recording was used to register neurometric data (spike rates across trials) from a chronically implanted microelectrode drive in the E1 barrel column.

Learning-related activity was then obtained from the slope of the regression of the smoothed learning score (from 0 to 1) and neuronal activities. A general tendency of decaying spike rates during CS presentation along with learning progress was found. This finding is comparable with the recent study of our group about TEBC learning, in which a similar experimental design was utilized (Silva-Prieto, Hofmann, and Schwarz 2023), making it likely that the S1 represents some aspects of learning in DEBC similar to TEBC. This finding is a first step towards elucidating the neuronal bases of the simultaneous and interactive nature of implicit and explicit learning systems in the mammalian brain. The concrete function of suppressed firing rates with increment in learning remains unclear and must be resolved in detail in future studies.

5 Deutsche Zusammenfassung

Der Lernerfolg bei EBC (Engl. Eyeblink conditioning) – ein Lidschluss evoziert durch einen vorher neutralen sensorischen Stimulus – wird klassischerweise dem unbewussten, Kleinhirn-abhängigen, impliziten/prozeduralen Gedächtnis zugeordnet, und kann ohne Beiträge des Großhirns erlernt werden. Menschen können jedoch die EBC Assoziation sprachlich beschreiben, und die daraus resultierenden bewussten Vorhersagen sind unabhängig vom prozeduralen Lernen, was die Überlegung aufwirft, dass selbst die einfachste Variante der Reflexkonditionierung die Großhirnrinde einbeziehen könnte, obwohl viele frühere Studien gezeigt haben, dass der prozedurale Teil des Lernens (d.h. das Erlernen der konditionierten Reaktionen, CRs) während Delayed-Conditioning (vielleicht die einfachste Form der klassischen Konditionierung) durch Blockade des Großhirns nicht beeinträchtigt wird (Oakley and Russell 1977; Mauk and Thompson 1987; Kronforst-Collins and Disterhoft 1998; Powell and Churchwell 2002).

Es gibt zwei Unterformen von EBC: Delayed-Eyeblink-Conditioning (DEBC) und Trace-Eyeblink-Conditioning (TEBC). Bei DEBC folgt sich der unkonditionierte Stimulus (US) mit einer Verzögerung auf den konditionierten Stimulus (CS), überlappt zeitlich mit ihm und endet gleichzeitig mit diesem. Bei Trace-Eyeblink-Conditioning (TEBC) gibt es ein stimulusfreies Intervall zwischen dem CS und dem US, was die Bildung einer Gedächtnisspur erfordert, um die beiden Reize zu verknüpfen. Es wurde gefunden, dass primärer somatosensorischer Kortex (S1, barrel cortex) bei Nagetieren lernabhängige Plastizitätsveränderungen während TEBC zeigte (Galvez et al. 2006; Galvez, Weible, and Disterhoft 2007a; Joachimsthaler et al. 2015) , während über seine Beteiligung während DEBC nur wenig bekannt ist. Aus diesem Grund versuchte die vorliegende Studie herauszufinden, ob es während des DEBC-Lernprozesses auch lernbezogene Plastizitätsveränderungen in S1 gibt. Wenn im S1 während der DEBC ähnliche Veränderungen wie bei der TEBC festgestellt werden könnten, würde dies die Auffassung unterstützen, dass es sich dabei um eine Folge eines expliziten Lernvorgangs handelt.

Zu diesem Zweck wurde kopffixierten wachen Mäusen als Versuchssubjekte verwendet, um während des gesamten Trainings und der Datenerfassung die höchste experimentelle Kontrolle zu gewährleisten. Mechanische Stimulation der E1 Vibrisse wurde als CS verwendet und ein Luftstoß gegen die Kornea des ipsilateralen Auges wurde als US verwendet. Während des gesamten Lernprozesses wurden die Lidschlussreaktionen registriert, um eine Lernkurve zu erstellen. Die Plastizitätsveränderungen wurden durch extrazelluläre Multi-Unit Feuerraten mittels chronsich implantierter Mikroelektroden in der E1 Barrel Kolumne registriert. Mithilfe von Matlab Programmen wurden local field potential (LFP) und Multi-Einheit Spikerate analysiert.

Die Spikerate wurde in Bezug auf den Lernerfolg (von 0 bis 1) dargestellt. Eine lineare Regressionsanalyse wurde verwendet, um die Beziehung zwischen den Veränderungen der neuronalen Aktivitäten und dem Lernfortschritt abzuschätzen. Es wurde die allgemeine Tendenz einer abnehmenden Spikerate während der CS-Präsentation parallel zum Lernfortschritt gefunden. Diese Feststellung steht im Einklang mit einer kürzlich durchgeführten Studie unseres Labors über TEBC-Lernen, bei der ein ähnliches experimentelles Design verwendet wurde (Silva-Prieto, Hofmann, and Schwarz 2023). Obwohl die Bedeutung und Funktion dieser neuronalen Aktivitätsunterdrückung nicht vollständig verstanden sind, ist es wahrscheinlich, dass der S1 einige Aspekte des assoziativen Lernens in DEBC ähnlich wie in TEBC repräsentiert. Diese Erkenntnis ist ein erster Schritt zur Aufklärung der neuronalen Grundlagen der gleichzeitigen und interaktiven Natur von impliziten und expliziten Lernsystemen im Säugetiergehirn.

6 Acknowledgment

First, I would like to express my deepest gratitude to Prof. Dr. Cornelius Schwarz for providing me with the chance to do my doctoral thesis in his lab. His insights and feedback were invaluable throughout the research process and his mentorship with great patience was crucial in shaping this work. Aside from my thesis, I appreciate him for offering me the opportunity to have an insight into fundamental research of neuroscience.

I also extend my gratitude to the members of my dissertation committee for attending my defense.

My research would not have been possible without the financial support from the Siegmund-Kiener-Stipendium, which allowed me to focus fully on my dissertation.

I must acknowledge my colleagues May Li Silva-Prieto and Kalpana Gupta for teaching me all I need to know about the experimental procedures so that I could start my independent work as soon as possible. I am also grateful for them patiently answering all my questions and giving me valuable suggestions.

Special thanks go to my family, who have provided me with phenomenal emotional support throughout this process. To my cats, Latte and Macchiato, and my boyfriend, Yimin Tong, for their endless patience, encouragement, and love, which were my sustenance on the days when the challenge seemed insurmountable.

Finally, I would like to express my gratitude to the staff at AG Schwarz for their assistance in accessing resources necessary for my research.

7 Statement of Authorship

I, the author, confirm that the work presented here has been performed and written solely by myself except where explicitly identified as the contrary. External thoughts and ideas as well as sources and other aids are made recognizable as such without exception.

7 Erklärung zum Eigenanteil

Die Arbeit wurde in Center of Integrative Neuroscience (CIN) and Hertie Institute for Clinical Neuroscience (HIH) unter Betreuung von Prof. Dr. rer. nat Cornelius Schwarz durchgeführt.
Die Konzeption der Studie erfolgte durch Prof. Dr. rer. nat Cornelius Schwarz.
Die sämtlichen Versuche wurden nach Einarbeitung durch Labormitglieder May Li Silva-Prieto and Kalpana Gupta von mir eigenständig durchgeführt. Die Datenanalyse inklusive Programmierung erfolgte größtenteils unter Unterstützung von Prof. Dr. rer. nat Cornelius Schwarz und May Li Silva-Prieto.
Ich versichere, das Manuskript selbständig verfasst zu haben und keine weiteren als die von mir angegebenen Quellen verwendet zu haben.

Tübingen, den 02.06.2024

8 References

Ahissar, E., R. Sosnik, K. Bagdasarian, and S. Haidarliu. 2001. 'Temporal frequency of whisker movement. II. Laminar organization of cortical representations', *J Neurophysiol*, 86: 354-67.

Ahissar, E., R. Sosnik, and S. Haidarliu. 2000. 'Transformation from temporal to rate coding in a somatosensory thalamocortical pathway', *Nature*, 406: 302-6.

Allen, M. T., Y. Padilla, and M. A. Gluck. 2002. 'Ibotenic acid lesions of the medial septum retard delay eyeblink conditioning in rabbits (Oryctolagus cuniculus)', *Behav Neurosci*, 116: 733-8.

Ammann, C., J. Marquez-Ruiz, M. A. Gomez-Climent, J. M. Delgado-Garcia, and A. Gruart. 2016. 'The Motor Cortex Is Involved in the Generation of Classically Conditioned Eyelid Responses in Behaving Rabbits', *J Neurosci*, 36: 6988-7001.

Armstrong-James, M., and C. A. Callahan. 1991. 'Thalamo-cortical processing of vibrissal information in the rat. II. spatiotemporal convergence in the thalamic ventroposterior medial nucleus (VPm) and its relevance to generation of receptive fields of S1 cortical "barrel" neurones', *J Comp Neurol*, 303: 211-24.

Armstrong-James, M., C. A. Callahan, and M. A. Friedman. 1991. 'Thalamo-cortical processing of vibrissal information in the rat. I. Intracortical origins of surround but not centre-receptive fields of layer IV neurones in the rat S1 barrel field cortex', *J Comp Neurol*, 303: 193-210.

Berry, S. D., and R. F. Thompson. 1979. 'Medial septal lesions retard classical conditioning of the nicitating membrane response in rabbits', *Science*, 205: 209-11.

Beylin, A. V., C. C. Gandhi, G. E. Wood, A. C. Talk, L. D. Matzel, and T. J. Shors. 2001. 'The role of the hippocampus in trace conditioning: temporal discontinuity or task difficulty?', *Neurobiol Learn Mem*, 76: 447-61.

Blankenship, M. R., R. Huckfeldt, J. J. Steinmetz, and J. E. Steinmetz. 2005. 'The effects of amygdala lesions on hippocampal activity and classical eyeblink conditioning in rats', *Brain Res*, 1035: 120-30.

Boele, H. J., S. K. Koekkoek, and C. I. De Zeeuw. 2010. 'Cerebellar and extracerebellar involvement in mouse eyeblink conditioning: the ACDC model', *Front Cell Neurosci*, 3: 19.

Brecht, M., and B. Sakmann. 2002a. 'Dynamic representation of whisker deflection by synaptic potentials in spiny stellate and pyramidal cells in the barrels and septa of layer 4 rat somatosensory cortex', *J Physiol*, 543: 49-70.

———. 2002b. 'Whisker maps of neuronal subclasses of the rat ventral posterior medial thalamus, identified by whole-cell voltage recording and morphological reconstruction', *J Physiol*, 538: 495-515.

Chakrabarti, S., and C. Schwarz. 2018. 'Cortical modulation of sensory flow during active touch in the rat whisker system', *Nat Commun*, 9: 3907.

Chmielowska, J., G. E. Carvell, and D. J. Simons. 1989. 'Spatial organization of thalamocortical and corticothalamic projection systems in the rat SmI barrel cortex', *J Comp Neurol*, 285: 325-38.

Christiansen, B. A., and N. A. Schmajuk. 1992. 'Hippocampectomy disrupts the topography of the rat eyeblink response during acquisition and extinction of classical conditioning', *Brain Res*, 595: 206-14.
Chung, S., X. Li, and S. B. Nelson. 2002. 'Short-term depression at thalamocortical synapses contributes to rapid adaptation of cortical sensory responses in vivo', *Neuron*, 34: 437-46.
Clark, R. E., J. R. Manns, and L. R. Squire. 2001. 'Trace and delay eyeblink conditioning: contrasting phenomena of declarative and nondeclarative memory', *Psychol Sci*, 12: 304-8.
Clark, R. E., and L. R. Squire. 1998. 'Classical conditioning and brain systems: the role of awareness', *Science*, 280: 77-81.
Crockett, D. P., D. W. Doherty, T. A. Henderson, M. M. Henegar, and M. F. Jacquin. 1995. 'Barrels VI: Proceedings of a satellite symposium of the 1994 Society for Neuroscience Meeting', *Somatosens Mot Res*, 12: 103-13.
Feldmeyer, D., M. Brecht, F. Helmchen, C. C. Petersen, J. F. Poulet, J. F. Staiger, H. J. Luhmann, and C. Schwarz. 2013. 'Barrel cortex function', *Prog Neurobiol*, 103: 3-27.
Fox, K., N. Wright, H. Wallace, and S. Glazewski. 2003. 'The origin of cortical surround receptive fields studied in the barrel cortex', *J Neurosci*, 23: 8380-91.
Furuta, T., T. Kaneko, and M. Deschenes. 2009. 'Septal neurons in barrel cortex derive their receptive field input from the lemniscal pathway', *J Neurosci*, 29: 4089-95.
Gallistel, C. R., S. Fairhurst, and P. Balsam. 2004. 'The learning curve: implications of a quantitative analysis', *Proc Natl Acad Sci U S A*, 101: 13124-31.
Galvez, R., A. P. Weible, and J. F. Disterhoft. 2007a. 'Cortical barrel lesions impair whisker-CS trace eyeblink conditioning', *Learn Mem*, 14: 94-100.
Galvez, R., C. Weiss, A. P. Weible, and J. F. Disterhoft. 2006. 'Vibrissa-signaled eyeblink conditioning induces somatosensory cortical plasticity', *J Neurosci*, 26: 6062-8.
Galvez, Roberto, Aldis P. Weible, and John F. Disterhoft. 2007b. 'Cortical barrel lesions impair whisker-CS trace eyeblink conditioning', *Learning & memory (Cold Spring Harbor, N.Y.)*, 14: 94-100.
Gdalyahu, A., E. Tring, P. O. Polack, R. Gruver, P. Golshani, M. S. Fanselow, A. J. Silva, and J. T. Trachtenberg. 2012. 'Associative fear learning enhances sparse network coding in primary sensory cortex', *Neuron*, 75: 121-32.
Gerdjikov, T. V., C. G. Bergner, and C. Schwarz. 2018. 'Global Tactile Coding in Rat Barrel Cortex in the Absence of Local Cues', *Cereb Cortex*, 28: 2015-27.
Ghazanfar, A. A., and M. A. Nicolelis. 1999. 'Spatiotemporal properties of layer V neurons of the rat primary somatosensory cortex', *Cereb Cortex*, 9: 348-61.
Goldreich, D., H. T. Kyriazi, and D. J. Simons. 1999. 'Functional independence of layer IV barrels in rodent somatosensory cortex', *J Neurophysiol*, 82: 1311-6.

Green, J. T., and J. D. Arenos. 2007. 'Hippocampal and cerebellar single-unit activity during delay and trace eyeblink conditioning in the rat', *Neurobiol Learn Mem*, 87: 269-84.
Gruart, A., P. Blazquez, and J. M. Delgado-Garcia. 1995. 'Kinematics of spontaneous, reflex, and conditioned eyelid movements in the alert cat', *J Neurophysiol*, 74: 226-48.
Gruart, A., B. G. Schreurs, E. D. del Toro, and J. M. Delgado-Garcia. 2000. 'Kinetic and frequency-domain properties of reflex and conditioned eyelid responses in the rabbit', *J Neurophysiol*, 83: 836-52.
Haiss, F., S. Butovas, and C. Schwarz. 2010. 'A miniaturized chronic microelectrode drive for awake behaving head restrained mice and rats', *J Neurosci Methods*, 187: 67-72.
Harris, J. A., R. S. Petersen, and M. E. Diamond. 1999. 'Distribution of tactile learning and its neural basis', *Proc Natl Acad Sci U S A*, 96: 7587-91.
Ivkovich, D., J. M. Lockard, and R. F. Thompson. 1993. 'Interpositus lesion abolition of the eyeblink conditioned response is not due to effects on performance', *Behav Neurosci*, 107: 530-2.
Ivkovich, D., C. M. Paczkowski, and M. E. Stanton. 2000. 'Ontogeny of delay versus trace eyeblink conditioning in the rat', *Dev Psychobiol*, 36: 148-60.
Jasinska, M., E. Siucinska, A. Cybulska-Klosowicz, E. Pyza, D. N. Furness, M. Kossut, and S. Glazewski. 2010. 'Rapid, learning-induced inhibitory synaptogenesis in murine barrel field', *J Neurosci*, 30: 1176-84.
Joachimsthaler, B., D. Brugger, A. Skodras, and C. Schwarz. 2015. 'Spine loss in primary somatosensory cortex during trace eyeblink conditioning', *J Neurosci*, 35: 3772-81.
Kronforst-Collins, M. A., and J. F. Disterhoft. 1998. 'Lesions of the caudal area of rabbit medial prefrontal cortex impair trace eyeblink conditioning', *Neurobiol Learn Mem*, 69: 147-62.
Land, P. W., and D. J. Simons. 1985. 'Metabolic and structural correlates of the vibrissae representation in the thalamus of the adult rat', *Neurosci Lett*, 60: 319-24.
Langer, D., M. van 't Hoff, A. J. Keller, C. Nagaraja, O. A. Pfaffli, M. Goldi, H. Kasper, and F. Helmchen. 2013. 'HelioScan: a software framework for controlling in vivo microscopy setups with high hardware flexibility, functional diversity and extendibility', *J Neurosci Methods*, 215: 38-52.
Lee, T., and J. J. Kim. 2004. 'Differential effects of cerebellar, amygdalar, and hippocampal lesions on classical eyeblink conditioning in rats', *J Neurosci*, 24: 3242-50.
Li, D. B., J. Yao, L. Sun, B. Wu, X. Li, S. L. Liu, J. M. Hou, H. L. Liu, J. F. Sui, and G. Y. Wu. 2019. 'Reevaluating the ability of cerebellum in associative motor learning', *Sci Rep*, 9: 6029.
Ma, P. M., and T. A. Woolsey. 1984. 'Cytoarchitectonic correlates of the vibrissae in the medullary trigeminal complex of the mouse', *Brain Res*, 306: 374-9.
Manns, I. D., B. Sakmann, and M. Brecht. 2004. 'Sub- and suprathreshold receptive field properties of pyramidal neurones in layers 5A and 5B of rat somatosensory barrel cortex', *J Physiol*, 556: 601-22.

Manns, J. R., R. E. Clark, and L. Squire. 2001. 'Single-cue delay eyeblink conditioning is unrelated to awareness', *Cogn Affect Behav Neurosci*, 1: 192-8.
Manns, J. R., R. E. Clark, and L. R. Squire. 2000a. 'Awareness predicts the magnitude of single-cue trace eyeblink conditioning', *Hippocampus*, 10: 181-6.
———. 2000b. 'Parallel acquisition of awareness and trace eyeblink classical conditioning', *Learn Mem*, 7: 267-72.
Maravall, M., R. S. Petersen, A. L. Fairhall, E. Arabzadeh, and M. E. Diamond. 2007. 'Shifts in coding properties and maintenance of information transmission during adaptation in barrel cortex', *PLoS Biol*, 5: e19.
Masino, S. A., M. C. Kwon, Y. Dory, and R. D. Frostig. 1993. 'Characterization of functional organization within rat barrel cortex using intrinsic signal optical imaging through a thinned skull', *Proc Natl Acad Sci U S A*, 90: 9998-10002.
Mauk, M. D., and R. F. Thompson. 1987. 'Retention of classically conditioned eyelid responses following acute decerebration', *Brain Res*, 403: 89-95.
McLaughlin, J., H. Skaggs, J. Churchwell, and D. A. Powell. 2002. 'Medial prefrontal cortex and pavlovian conditioning: trace versus delay conditioning', *Behav Neurosci*, 116: 37-47.
Miller, D. B., M. M. Rassaby, K. A. Collins, and M. R. Milad. 2022. 'Behavioral and neural mechanisms of latent inhibition', *Learn Mem*, 29: 38-47.
Minnery, B. S., R. M. Bruno, and D. J. Simons. 2003. 'Response transformation and receptive-field synthesis in the lemniscal trigeminothalamic circuit', *J Neurophysiol*, 90: 1556-70.
Mitzdorf, U. 1985. 'Current source-density method and application in cat cerebral cortex: investigation of evoked potentials and EEG phenomena', *Physiol Rev*, 65: 37-100.
Moyer, J. R., Jr., R. A. Deyo, and J. F. Disterhoft. 1990. 'Hippocampectomy disrupts trace eye-blink conditioning in rabbits', *Behav Neurosci*, 104: 243-52.
Nicholson, C., and J. A. Freeman. 1975. 'Theory of current source-density analysis and determination of conductivity tensor for anuran cerebellum', *J Neurophysiol*, 38: 356-68.
Oakley, D. A., and I. S. Russell. 1972. 'Neocortical lesions and Pavlovian conditioning', *Physiol Behav*, 8: 915-26.
———. 1975. 'Role of cortex in Pavlovian discrimination learning', *Physiol Behav*, 15: 315-21.
———. 1977. 'Subcortical storage of Pavlovian conditioning in the rabbit', *Physiol Behav*, 18: 931-7.
Ohno, S., E. Kuramoto, T. Furuta, H. Hioki, Y. R. Tanaka, F. Fujiyama, T. Sonomura, M. Uemura, K. Sugiyama, and T. Kaneko. 2012. 'A morphological analysis of thalamocortical axon fibers of rat posterior thalamic nuclei: a single neuron tracing study with viral vectors', *Cereb Cortex*, 22: 2840-57.
Oswald, B., B. Knuckley, K. Mahan, C. Sanders, and D. A. Powell. 2006. 'Prefrontal control of trace versus delay eyeblink conditioning: role of the

unconditioned stimulus in rabbits (Oryctolagus cuniculus)', *Behav Neurosci*, 120: 1033-42.
Papka, Michelle, Richard B. Ivry, and Diana S. Woodruff-Pak. 1997. 'Eyeblink Classical Conditioning and Awareness Revisited', *Psychological Science*, 8: 404-08.
Pavlov, P. I. 2010. 'Conditioned reflexes: An investigation of the physiological activity of the cerebral cortex', *Ann Neurosci*, 17: 136-41.
Perruchet, P. 1985. 'A pitfall for the expectancy theory of human eyelid conditioning', *Pavlov J Biol Sci*, 20: 163-70.
Port, R. L., A. A. Mikhail, and M. M. Patterson. 1985. 'Differential effects of hippocampectomy on classically conditioned rabbit nictitating membrane response related to interstimulus interval', *Behav Neurosci*, 99: 200-8.
Powell, D. A., and J. Churchwell. 2002. 'Mediodorsal thalamic lesions impair trace eyeblink conditioning in the rabbit', *Learn Mem*, 9: 10-7.
Puga, F., D. W. Barrett, C. C. Bastida, and F. Gonzalez-Lima. 2007. 'Functional networks underlying latent inhibition learning in the mouse brain', *Neuroimage*, 38: 171-83.
Sakamoto, T., and S. Endo. 2010. 'Amygdala, deep cerebellar nuclei and red nucleus contribute to delay eyeblink conditioning in C57BL /6 mice', *Eur J Neurosci*, 32: 1537-51.
Schade Powers, A., P. Coburn-Litvak, and C. Evinger. 2010. 'Conditioned eyelid movement is not a blink', *J Neurophysiol*, 103: 641-7.
Schwarz, C., H. Hentschke, S. Butovas, F. Haiss, M. C. Stuttgen, T. V. Gerdjikov, C. G. Bergner, and C. Waiblinger. 2010. 'The head-fixed behaving rat--procedures and pitfalls', *Somatosens Mot Res*, 27: 131-48.
Siegel, J. J., W. Taylor, R. Gray, B. Kalmbach, B. V. Zemelman, N. S. Desai, D. Johnston, and R. A. Chitwood. 2015. 'Trace Eyeblink Conditioning in Mice Is Dependent upon the Dorsal Medial Prefrontal Cortex, Cerebellum, and Amygdala: Behavioral Characterization and Functional Circuitry', *eNeuro*, 2.
Silva-Prieto, M. L., J. I. Hofmann, and C. Schwarz. 2023. 'Activity in Barrel Cortex Related to Trace Eyeblink Conditioning', *eNeuro*, 10.
Simons, D. J. 1985. 'Temporal and spatial integration in the rat SI vibrissa cortex', *J Neurophysiol*, 54: 615-35.
Solomon, P. R., E. R. Vander Schaaf, R. F. Thompson, and D. J. Weisz. 1986. 'Hippocampus and trace conditioning of the rabbit's classically conditioned nictitating membrane response', *Behav Neurosci*, 100: 729-44.
Stuttgen, M. C., J. Ruter, and C. Schwarz. 2006. 'Two psychophysical channels of whisker deflection in rats align with two neuronal classes of primary afferents', *J Neurosci*, 26: 7933-41.
Stuttgen, M. C., and C. Schwarz. 2008. 'Psychophysical and neurometric detection performance under stimulus uncertainty', *Nat Neurosci*, 11: 1091-9.
———. 2010. 'Integration of vibrotactile signals for whisker-related perception in rats is governed by short time constants: comparison of neurometric and psychometric detection performance', *J Neurosci*, 30: 2060-9.

Takehara-Nishiuchi, K. 2018. 'The Anatomy and Physiology of Eyeblink Classical Conditioning', *Curr Top Behav Neurosci*, 37: 297-323.
Takehara, K., S. Kawahara, and Y. Kirino. 2003. 'Time-dependent reorganization of the brain components underlying memory retention in trace eyeblink conditioning', *J Neurosci*, 23: 9897-905.
Taub, A. H., and M. Mintz. 2010. 'Amygdala conditioning modulates sensory input to the cerebellum', *Neurobiol Learn Mem*, 94: 521-9.
Thompson, R. F., S. Bao, L. Chen, B. D. Cipriano, J. S. Grethe, J. J. Kim, J. K. Thompson, J. A. Tracy, M. S. Weninger, and D. J. Krupa. 1997. 'Associative learning', *Int Rev Neurobiol*, 41: 151-89.
Tseng, W., R. Guan, J. F. Disterhoft, and C. Weiss. 2004. 'Trace eyeblink conditioning is hippocampally dependent in mice', *Hippocampus*, 14: 58-65.
Umeda, T., T. Isa, and Y. Nishimura. 2019. 'The somatosensory cortex receives information about motor output', *Sci Adv*, 5: eaaw5388.
Veinante, P., and M. Deschenes. 1999. 'Single- and multi-whisker channels in the ascending projections from the principal trigeminal nucleus in the rat', *J Neurosci*, 19: 5085-95.
Veinante, P., P. Lavallee, and M. Deschenes. 2000. 'Corticothalamic projections from layer 5 of the vibrissal barrel cortex in the rat', *J Comp Neurol*, 424: 197-204.
Waiblinger, C., D. Brugger, and C. Schwarz. 2015. 'Vibrotactile discrimination in the rat whisker system is based on neuronal coding of instantaneous kinematic cues', *Cereb Cortex*, 25: 1093-106.
Wang, Q., R. M. Webber, and G. B. Stanley. 2010. 'Thalamic synchrony and the adaptive gating of information flow to cortex', *Nat Neurosci*, 13: 1534-41.
Webber, R. M., and G. B. Stanley. 2006. 'Transient and steady-state dynamics of cortical adaptation', *J Neurophysiol*, 95: 2923-32.
Weible, A. P., M. D. McEchron, and J. F. Disterhoft. 2000. 'Cortical involvement in acquisition and extinction of trace eyeblink conditioning', *Behav Neurosci*, 114: 1058-67.
Weidemann, G., M. Satkunarajah, and P. F. Lovibond. 2016. 'I Think, Therefore Eyeblink: The Importance of Contingency Awareness in Conditioning', *Psychol Sci*, 27: 467-75.
Weiskrantz, L., and E. K. Warrington. 1979. 'Conditioning in amnesic patients', *Neuropsychologia*, 17: 187-94.
Weiss, C., and J. F. Disterhoft. 2008. 'Evoking blinks with natural stimulation and detecting them with a noninvasive optical device: a simple, inexpensive method for use with freely moving animals', *J Neurosci Methods*, 173: 108-13.
Welker, C. 1976. 'Receptive fields of barrels in the somatosensory neocortex of the rat', *J Comp Neurol*, 166: 173-89.
Willmore, B. D., J. A. Mazer, and J. L. Gallant. 2011. 'Sparse coding in striate and extrastriate visual cortex', *J Neurophysiol*, 105: 2907-19.
Wimmer, V. C., R. M. Bruno, C. P. de Kock, T. Kuner, and B. Sakmann. 2010. 'Dimensions of a projection column and architecture of VPM and POm axons in rat vibrissal cortex', *Cereb Cortex*, 20: 2265-76.

Woolsey, T. A., and H. Van der Loos. 1970. 'The structural organization of layer IV in the somatosensory region (SI) of mouse cerebral cortex. The description of a cortical field composed of discrete cytoarchitectonic units', *Brain Res*, 17: 205-42.
Wright, N., and K. Fox. 2010. 'Origins of cortical layer V surround receptive fields in the rat barrel cortex', *J Neurophysiol*, 103: 709-24.
Wu, G. Y., J. Yao, B. Hu, H. M. Zhang, Y. D. Li, X. Li, Q. Li, and J. F. Sui. 2013. 'Reevaluating the role of the hippocampus in delay eyeblink conditioning', *PLoS One*, 8: e71249.
Wu, G. Y., J. Yao, L. Q. Zhang, X. Li, Z. L. Fan, Y. Yang, and J. F. Sui. 2012. 'Reevaluating the role of the medial prefrontal cortex in delay eyeblink conditioning', *Neurobiol Learn Mem*, 97: 277-88.
Yang, H., and D. H. O'Connor. 2014. 'Cortical adaptation and tactile perception', *Nat Neurosci*, 17: 1434-6.